

LOW SPEED BOUNDARY LAYER AND PRESSURE  
DISTRIBUTION TESTS ON A FAMILY OF  
SWEEP BACK WINGS

Thesis by  
Harvey O. Nay

In Partial Fulfillment of the Requirements  
For the Degree of  
Aeronautical Engineer

California Institute of Technology  
Pasadena, California

1952

## ACKNOWLEDGEMENTS

The author wishes to express his appreciation for the aid and guidance given him by Dr. Clark B. Millikan, under whose supervision this investigation was carried out. He also extends his thanks to all of the many persons at the California Institute and at the Douglas Company who have helped with the work in various ways. A special debt of gratitude is owed by the author to the following persons at the Douglas Company: Mr. K. E. Van Every, for suggesting the project and for his guidance as the work progressed; Mr. A. M. C. Smith, for many valuable suggestions and helpful criticisms; Mr. B. W. Marsh, for his aid in carrying out the investigation; Mr. R. D. Hager, for doing the detail design of the equipment; and Mr. R. C. Leeds, Miss Kathryn Smith and Mrs. Doris Rothermel, for their help in the testing, reduction of data, etc. A special word of thanks is due Mrs. Helena Marsh for her work on the illustrations. The author is also very grateful to the Douglas Aircraft Company for their permission to use the data presented herein.

## ABSTRACT

Low-speed tests were conducted to determine boundary layer and surface pressure distribution characteristics of a systematic family of swept back wings. It is intended that the test results will have application in giving a better understanding of the viscous flow phenomena on swept back wings, particularly in relation to the stall. A general picture of the boundary layer flow and surface pressure distribution at high lift conditions, showing the effects of variations in wing planform, was determined. Several existing concepts were verified and an attempt was made to define the limits of applicability of these concepts.

A localized separation of the flow perpendicular to the leading edge of the wing, hereinafter referred to as the "normal flow", was found to occur at lift coefficients somewhat below the stall on the wings with appreciable sweepback. The separation took the form of a vortex streak running aft and outboard from an origin near the leading edge, and it greatly affected the boundary layer structure and the surface pressure distribution.

Generalization of surface pressure distribution on the basis of the local lift coefficient and dynamic pressure for the normal flow was found to hold fairly well for the various sweepback angles.

The development of stall was determined for the various planforms in terms of boundary layer thickness and flow direction near the surface of the wing.

Generalization of the shape of the profiles of the normal boundary layer flow component in terms of a single family of shapes for all sweepback angles, as suggested by other researchers, was shown to be possible.

## TABLE OF CONTENTS

<u>Part</u>	<u>Title</u>	<u>Page</u>
	Acknowledgements	
	Abstract	
	Table of Contents	
	Index to Figures	
	Notation	
I	Introduction	1
II	Experimental Apparatus	11
III	Tests and Analysis of the Data	16
IV	Experimental Results	20
V	Conclusions	29
VI	References	31
	Figures 1-22	32-53

## INDEX TO FIGURES

<u>Figure</u>	<u>Title</u>	<u>Page</u>
1.	Douglas El Segundo Wind Tunnel	32
2.	Wing Model	33
3.	Test Installation	34
4.	Boundary Layer Instrument	35
5.	Boundary Layer Velocity Profiles on Wind Tunnel Wall	36
6.	Effects of Transition Strip Size on Boundary Layer Profiles	37
7.	Repeatability of Data	38
8.	Effect of Sweepback and Angle of Attack on Surface Pressure Distribution--Aspect Ratio = 6	39
9.	Effect of Aspect Ratio and Angle of Attack on Surface Pressure Distribution--Sweepback = $35^\circ$	40
10.	Local Section Lift Curves	41
11.	Spanwise Distribution of Lift	42
12.	Lift Curves for Various Wing Planforms	43
13.	Resolution of Surface Pressure Distribution	44
Boundary Layer Thickness and Flow Direction Near Wing Surface:		
14.	Angle of attack = $4^\circ$	45
15.	Angle of Attack = $8^\circ$	46
16.	Angle of Attack = $10^\circ$	47
17.	Angle of Attack = $12^\circ$	48
Generalization of Boundary Layer Profile Shape:		
18.	Sweepback = $0^\circ$ Aspect Ratio = 6	49
19.	Sweepback = $20^\circ$ Aspect Ratio = 6	50
20.	Sweepback = $35^\circ$ Aspect Ratio = 6	51
21.	Sweepback = $45^\circ$ Aspect Ratio = 6	52
22.	Effect of Sweepback on Generalization of Boundary Layer Profile Shape	53

## NOTATION

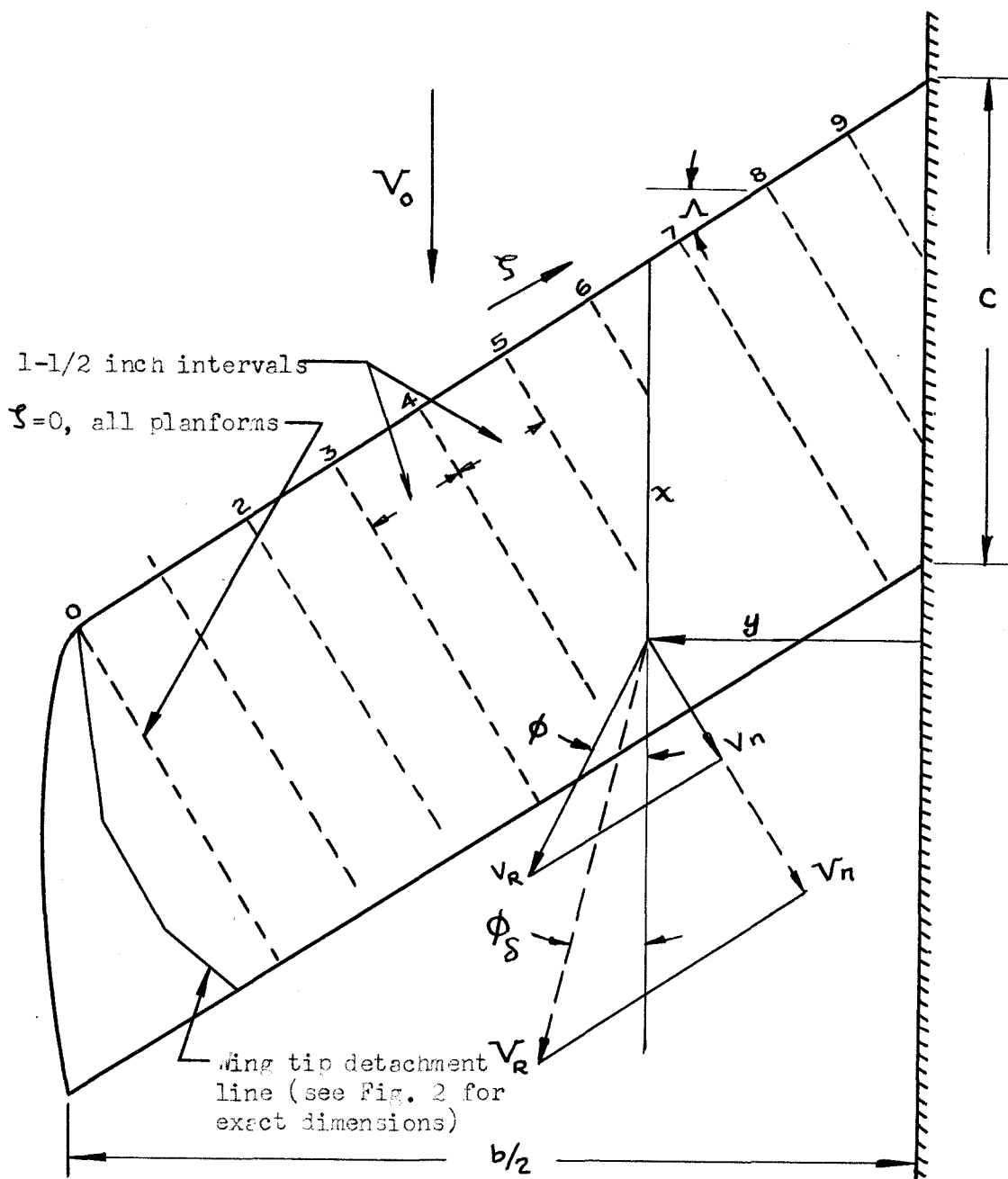
### Symbols

$R$	aspect ratio ( $b^2/s$ )
$b$	span of complete wing ft.
$c$	wing chord measured in wind stream direction ft.
$C_p$	static pressure coefficient ( $\frac{p-p_o}{q_o}$ )
$C_{pt}$	total pressure coefficient ( $\frac{p_t-p_o}{q_o}$ )
$C_l$	local section lift coefficient ( $\int_0^1 (C_{pp} - C_{ps}) d(x/c)$ )
$C_L$	wing lift coefficient ( $\int_0^1 C_l d(\frac{y}{b/2})$ )
$H$	boundary layer profile shape parameter ( $S^*/\theta$ )
$p$	static pressure lb/ft <sup>2</sup>
$p_t$	total pressure lb/ft <sup>2</sup>
$q$	dynamic pressure lb/ft <sup>2</sup>
$S$	wing plan area ft <sup>2</sup>
$v$	local velocity ft/sec
$V$	velocity at edge of boundary layer ft/sec
$V_o$	free-stream velocity ft/sec
$x$	chordwise coordinate parallel to free stream ft.
$y$	spanwise coordinate perpendicular to free stream ft.
$z$	distance measured perpendicular to wing surface ft.
$\alpha$	angle of attack measured in plane of wind tunnel wall degrees
$\delta$	boundary layer thickness in.
$\delta^*$	boundary layer displacement thickness ( $\int_0^{\delta} (1 - \frac{v}{V}) dz$ ) in.
$\xi$	spanwise coordinate parallel to wing leading edge-(see sketch below)
$\theta$	boundary layer momentum thickness ( $\int_0^{\delta} (1 - \frac{v}{V}) \frac{v}{V} dz$ ) in.
$\Lambda$	sweepback angle degrees
$\phi$	flow direction angle (see sketch below) degrees

Subscripts

- n component normal to wing leading edge
- p pressure surface of wing
- o free stream
- R resultant
- s suction surface of wing
- $\delta$  at edge of boundary layer

Dimensional Notation



## I INTRODUCTION

### General Background

Accompanying the improvements in the transonic drag of aircraft brought about by increasing the sweepback of the wings are some undesirable effects, one of which is the deterioration of longitudinal stability at the stall as the sweepback is increased. In the design of swept back wings the problem of stalling stability is a serious one, and several devices are in current use to counteract adverse sweepback effects. These devices, although effective, are not entirely satisfactory because of their mechanical complication, weight, and drag. The Douglas Aircraft Company has undertaken a program to develop more efficient swept back wing configurations with satisfactory stall characteristics. As the first phase of this program, tests were made in order to gain a better understanding of the basic phenomena of swept-wing boundary layer flow. The results presented in this thesis are from these first-phase tests, which consisted of static pressure, velocity, and flow direction measurements in the boundary layer on a systematic family of swept back wings.

### The Problem of Longitudinal Stability at the Stall with Swept Back Wings

The poor stability characteristics of swept back wings at the stall are caused by the separation of the flow occurring first at the tips of the wings, causing the center of pressure to move forward. This results in a pitching moment tending to further increase the angle of attack and aggravate the stall. Thus, as the stall develops at the tips, there is a tendency for angle of attack to increase sharply in an unstable, divergent manner. The magnitude of the de-stabilizing moment at the stall depends on many factors, but the most important for wings without special stall control devices, are the sweepback and aspect ratio. The effects



of these parameters on stalling stability are discussed in Reference 1. In general, the stability problem is made more severe by an increase in either sweepback or aspect ratio.

The reason for the separation of flow occurring first at the tips of swept back wings can be understood by considering the spanwise distribution of lift and the flow in the boundary layer. The results of lift distribution calculations show that as wing sweepback is increased, the loading of the outboard portion of the wing increases with respect to the center section. With more of the load carried outboard, a swept back wing must have a larger effective angle of attack on the outboard section as compared with the inboard section than does a straight wing. Thus, the swept back wing has more of a tendency to stall first at the tips than does a straight wing. The pressure field on a swept back wing tends to cause the low-energy air in the boundary layer to flow outboard in the region where the pressure is increasing in the downstream direction. The out-flow of air in the boundary layer of a swept back wing delays the stall of the portion of the wing well inboard from the tips. This occurs because the adverse pressure gradient in the direction of boundary layer flow is less with the out-flow than would be present if the boundary layer flowed directly back to the trailing edge with no out-flow. As the wing tip is approached, the effect of the high pressure on the lower surface of the wing makes itself felt on the upper surface to an increasingly large extent, corresponding to the sharp drop-off in lift very near the tip. The sharp increase in pressure causes the air just inboard of the tips to decelerate, and this causes a piling-up of low-energy air near the tips, which leads to early separation as the angle of attack is increased.

By using special devices tip stall can be delayed to higher angles of attack than the stalling angle for the inboard section, thus making it possible to preserve longitudinal stability at the stall, even for high-aspect-ratio, highly swept back wings. The device most commonly used to prevent tip stall on swept back wings is a retractable slat on the outboard wing section, usually operated aerodynamically to open at high lift coefficients. The action of slats in delaying separation is that of mixing a high-energy jet of air with the low-energy boundary layer, thus distributing the energy decrement over a larger thickness and increasing the velocity of the air next to the surface. Slats can also be used to increase the maximum lift of a wing; however, they are not very effective in this when used to obtain stability at the stall. Slats are complicated, both mechanically and aerodynamically, and add weight and drag to an airplane; therefore, it is felt that they are not very satisfactory devices when used to obtain stalling stability with swept back wings. Plates projecting vertically from the upper surface of the wing and parallel to the flight direction have been used to prevent spanwise boundary layer flow and aid in delaying tip stall on wings with sweepback. These devices, which are called stall plates, are not as effective as slats and they have the disadvantage of counteracting, to some extent, the effect of wing sweepback in reducing high-speed drag.

Other devices that show promise for controlling stall include combined variations in wing incidence and airfoil section shape along the span, variations in wing planform, and the use of boundary layer control. Vortex generators (protuberances on the wing surfaces used to create chordwise running vortices) should delay stall to higher lift by mixing high-energy air with the boundary layer in a manner similar to the action of slats.

Existing Concepts and Experimental Results on Pressure Distribution and Boundary Layer Structure on Swept Back Wings

The most elementary approach to the analysis of flow phenomena around swept back wings is what is usually referred to as the simple sweep theory. This concept is derived by considering the flow around a yawed cylindrical body of infinite span in non-viscous flow. It can be seen that the pressure field is the same as it would be if only the normal flow were present. In this case the component of velocity parallel to the body is constant and has no effect on the pressure distribution. Stated symbolically, the pressures at corresponding points on a swept and on an unswept body are related by

$$C_{p\Lambda} = C_{p\Lambda=0} \cos^2 \Lambda \quad \text{for} \quad \alpha_{\Lambda} = \alpha_{\Lambda=0} \cos \Lambda.$$

This simple concept is responsible for the initial investigations of the use of sweepback as a means of delaying transonic drag rise.

Since the pressure field outside the boundary layer is nearly independent of viscous effects except for flows involving large regions of separation, the assumption of non-viscous flow in the derivation of the simple sweep theory for pressure distribution does not seriously limit its applicability for low and intermediate lift conditions. However, the assumption of infinite span causes a serious limitation on the applicability of the simple sweep theory to actual wings, because the pressure field is greatly affected by spanwise variations in lift and by the special flow configurations at the root and tip. Variations in pressure distribution along the span at zero lift are shown in Reference 2 for an unswept and 40-degree-swept back wing. It can be seen from the test results reported in this reference that the effect of sweepback is to shift the peak negative pressure aft near the root and forward near the tip. This

phenomenon of pressure distribution shift can be predicted by consideration of the condition that the flow at the root and tip must be in the direction of the free stream.

The spanwise pressure gradient due to lift on a finite wing can be obtained by the consideration of the lift distribution on an actual wing. (The reader is referred to the extensive literature on the subject of lift distribution). It can be noted that the spanwise pressure gradient due to lift will increase with the lift itself and will decrease with increasing aspect ratio.

The validity of the simple sweep theory in application to finite wings is seen to be rather limited, especially for low-aspect-ratio wings and for high lift. Some improvement of the simple sweep theory is possible by the generalization of the pressure field in terms of the local section lift coefficient based on the normal flow. Symbolically,

$$C_{p\Lambda} = C_{p\Lambda=0} \cos^2 \Lambda. \quad \text{for } C_{l\Lambda} = C_{l\Lambda=0} \cos^2 \Lambda.$$

This generalization should be applicable to that portion of the wing sufficiently far from the root and tip that the longitudinal shift in the pressure pattern is small. It is possible using this concept to calculate the pressure distribution over a swept back wing from airfoil section data and from a knowledge of the spanwise lift distribution, which can be calculated readily using widely accepted existing theory. There remains the question of the modification necessary due to the root and tip effects and the definition of the limits of applicability of this approach and the effects of exceeding these limits.

The desirability of establishing some simplifying principles by which swept-wing boundary layer flow could be treated in a manner analogous to the simple sweep theory for pressure distribution is apparent.

Prandtl in Reference 3 has discussed such an approach and has shown that the component of boundary layer flow perpendicular to the axis of a yawed infinite cylinder in laminar flow would be independent of the flow parallel to the axis. In References 4 and 5 Sears and Wild have used this principle in obtaining solutions for the boundary layer growth and flow direction on a flat plate and an elliptical cylinder. They have each shown for the laminar-flow cases they considered that the normal flow about infinite-span bodies is independent of the angle of yaw.

For the cases of flow involving turbulence or wakes, it is not possible to show mathematically the non-dependence of the normal boundary layer flow on yaw as was done for laminar flow. However, Jones has examined the general case of flow about a yawed infinite cylinder from purely physical considerations (Reference 6) and has concluded that the simple sweep theory for boundary layer should be applicable to the normal flow in cases involving turbulence and separation as well as in the laminar-flow case. He presents experimental verification of this concept in the form of drag data on a circular wire at various yaw angles at sub-critical Reynolds numbers of  $10^2$  to  $10^3$ . Results from recent tests on yawed circular cylinders in the critical Reynolds number range are reported in Reference 7. These tests showed large effects of yaw on critical Reynolds number and super-critical drag coefficient based on the normal flow. This shows that the hypothesis of the simple sweep theory holding for flows involving separation and a large wake is not valid for Reynolds numbers above the critical on circular cylinders. It would seem, however, that for wings below the stall, discrepancies from the simple sweep theory may be much smaller due to the much smaller wake.

The effect of turbulent boundary layer on the validity of the simple sweep theory was unknown at the time the subject tests were made. However, a recent report (Reference 8) shows a comparison of a straight wing and a 45-degree-swept wing with turbulent boundary layer (Reynolds number based on the normal flow = approximately four million). Both wings completely spanned the wind tunnel and were designed to have minimum spanwise pressure gradients. The test results showed excellent verification of the simple sweep theory in relating the normal boundary layer flow between 0 and 45 degrees of sweepback up to the highest lift coefficients tested, which were somewhat below the stall.

The spanwise variations in pressure that arise in the case of an actual wing would be expected to cause some variation in the characteristics of the perpendicular boundary layer with changes in spanwise station, contrary to the simple sweep theory. The idea arises that an extension of the simple sweep theory similar to the extension mentioned above for the pressure distribution may make it possible to determine the normal component of boundary layer flow on the basis of the local lift coefficient and dynamic pressure, both based on the normal component of the free-stream flow. In order to establish the validity of this approach it would be necessary to establish two principles, namely, that the family of shapes that the normal boundary layer velocity profile can assume as the "fullness" is varied by pressure gradients is the same regardless of sweepback, and that the effects of pressure gradients in the normal direction on the profile shape does not vary with sweepback. The discussion of these two principles will be restricted here to the case of turbulent boundary layer because it is of primary interest in the problem under consideration.

The family of shapes that the turbulent boundary layer velocity profile can assume and the approximate effects of pressure gradient on the

shape were determined for straight wings by von Doenhoff and Tetervin as reported in Reference 9. It was shown that the profile shape can be described by a single shape parameter  $H$ , which is the ratio of the displacement to the momentum thickness. An empirical formula was obtained relating the shape parameter to the initial shape and momentum thickness and the pressure gradient. The results presented are based on a considerable number of tests of airfoils and other shapes. The variation in profile shape with the shape parameter is also presented in Reference 10. The latter variation was obtained from tests on a specially designed large-scale two-dimensional body, and although there are some slight systematic discrepancies agreement with the results presented in Reference 9 is quite good. It is concluded that the family of possible turbulent boundary layer profiles is established with reasonable engineering accuracy for unswept bodies.

Turbulent boundary layer profile shape variation for the normal flow is available for a 20-degree-swept back wing of aspect ratio about 4.5 in Reference 11. The generalization of the profile shape in terms of the shape parameter shown is essentially the same as the generalizations of References 9 and 10 for straight, two-dimensional shapes. Because the sweepback angle was small, however, it is not possible to conclude from the results of Reference 11 that the normal velocity profile is independent of sweepback and spanwise pressure gradients.

Localized separation of a laminar boundary layer followed by transition of the detached flow and re-attachment of the resulting turbulent boundary layer has been observed in many instances over the past twenty years. This phenomenon, which is generally referred to as laminar "bubble" formation, is discussed in detail in a recent report (Reference 12).

No complete analysis of the "bubble" problem has yet been made, but it is known to lead to appreciable changes in the pressure distribution and increases in the rate of change of lift with angle of attack. The effect of sweepback on localized laminar separation is not available, but it would certainly be expected to prove a serious limitation to any known method of analyzing pressure distribution or boundary layer on swept back wings.

The methods of analysis and the generalizations mentioned above shed a great deal of light on the picture of boundary layer flow phenomena. In certain special cases it is possible to determine accurately the flow field on a swept back body. However, the limits of applicability of the various concepts are not well established, and there is not sufficient information to establish good general ideas of what happens when the limits of applicability are exceeded. Some of the concepts which appear promising for use in swept wing flow analysis need further verification to establish their validity.

#### Purposes of the Tests Reported Herein

In order to apply some of the more promising stall control devices in the development of swept back wing configurations with satisfactory stall characteristics and with less weight and drag than present designs, more information is needed on the general nature of boundary layer flow and pressure distribution. The tests reported here were made to supply some of this general information and to check concepts that had been previously advanced. It was felt that the amount of testing necessary to find satisfactory configurations could be greatly reduced if sufficient generalizations could be made from the results of simple tests such as these. In relation to the actual design problem of obtaining satisfactory



pitching-moment variation at the stall, the subject tests are concerned only with that part of the problem associated with the separation of flow that causes stall. This report does not consider the effects of the character of the stall on the pitching moment or the question of what constitutes satisfactory pitching-moment variation.

Specifically, the tests reported in this thesis were made for the following purposes:

1. To determine the variation with sweepback and aspect ratio of wing surface pressure distribution as a function of angle of attack. It was felt that this information would give a general insight into the character of stall development and would provide an essential part, along with measurements of flow direction and boundary layer thickness, of the picture of causes and effects of changes in boundary layer flow with angle of attack.
2. To determine regions of applicability of the use of the refined simple sweep theory in determining pressure distribution.
3. To compare theoretical and actual span load distribution to gain insight into stall development by noting variations with wing planform of the deviation between the two.
4. To determine the flow direction in the boundary layer for the various planforms.
5. To determine variations in boundary layer thickness for various planforms.
6. To determine generalized boundary layer characteristics to compare with previous generalizations for straight wings and to determine if straight-wing generalizations can be extended to swept back wings.

## II EXPERIMENTAL APPARATUS

### Wind Tunnel

The low-speed wind tunnel at the El Segundo Division of the Douglas Aircraft Company, Inc. was used for the testing. A sketch of this wind tunnel is given in Figure 1. It is of the closed-return type, operating at atmospheric pressure, and capable of producing wind velocities up to 250 ft/sec in the 30- by 45-inch test section. For the present tests a tunnel boundary layer bleed was provided on one of the walls of the test section, where the model was mounted. The boundary layer air that was bled from the tunnel was drawn off by an auxiliary blower.

### Model and Installation

One wing model, having an NACA 63<sub>1</sub>-012 airfoil section perpendicular to the leading edge, was used throughout the tests. The wing had a chord of six inches and was not tapered. It was mounted as a reflection plane (half-span) model on the wall of the test section. Various planforms were obtained by sliding the wing in and out of the test section and rotating it about a vertical axis. A sketch of the model is given in Figure 2. The wing core was made of steel and the surface of mahogany.

Copper tubes running spanwise were fitted for use in the measurement of surface static-pressure distribution. The tubes were installed projecting slightly beyond the wing contour and were filed down flush with the surface, each tube leaving a copper strip about one-half the tube diameter wide in the wing surface. Holes were drilled in the tubes at 1 1/2 inch intervals along the span. The ends of the tubes at the wing tip were sealed off and the tubes were led out to a manometer board through the root end of the wing.

The wing was fitted with a different tip for each angle of sweep-back. The tip fairings were rounded in front view, and in each case the

line of intersection of the tip fairing and the basic wing was parallel to the wind stream. A roughness strip about  $3/16$  inch wide was attached to the wing at  $7\ 1/2$  percent of the chord from the leading edge to fix boundary layer transition. Two transition strips were used in the course of the tests; both were obtained by removing the paper from the back of regular commercial sandpaper. The first strip used was obtained from No. 2 sandpaper and projected about 0.018 inch from the wing surface. For the latter part of the tests the transition strip was obtained from No. 1/0 sandpaper and projected about 0.010 inch.

The model was projected into the wind tunnel through a hole in the side of the test section and was supported by structure outside the wind tunnel. The hole where the wing passed through the tunnel wall was faired out and sealed off so that the wing was effectively mounted on a reflection plane. The wing was clamped to a heavy plate, which could be rotated to change the angle of attack of the model. Variation of angle of attack was accomplished by movement of a lever attached to the heavy plate on which the model was mounted. The other end of the lever was clamped to the supporting structure to hold the wing in position when angle of attack was set.

The wing extended into the tunnel through a hole cut in a circular disc which made up part of the test section wall. This circular disc was attached to the same plate on which the model was clamped and rotated with the model when angle of attack was changed. The zero angle of attack position of the wing was determined by varying the angle until the pressures measured on the upper and lower surfaces of the wing were equal. A protractor scale was then marked on the circular plate in the side of the tunnel from which other angle of attack settings could be determined.

The test installation is illustrated in Figure 3.

### Instrumentation

Static pressure distribution on the wing surface was measured by means of the spanwise-running tubes mentioned in the description of the model. The tubes were sealed at the tip end and passed out of the test section through the root end, whence they were connected to a multiple-tube manometer. Small holes were drilled in each tube at frequent intervals along the span. Pressure distribution data were obtained by sealing off with Scotch tape all but one hole in each tube, determining the pressure at points where the holes were uncovered, changing the tape to uncover a new set of holes, and repeating the process until all the desired data were obtained.

Total pressure and flow direction in the boundary layer were measured by an instrument designed and built especially for these tests. A sketch of this instrument is shown in Figure 4, and it can be seen in operating position below the wing in Figure 3. The instrument itself consisted of two basic parts, a structural body of 3/4-inch pipe and a central shaft which could be rotated and moved vertically inside the structural body and on which the pick-up head was mounted. The instrument projected through the tunnel floor and the operator manipulated it and took readings from a point below the test section.

A movable mounting in the floor of the test section was provided for the instrument so that it could be shifted to various positions on the surface of the model. The upper part of the structural body of the instrument ended in a cork-padded "foot", which was off-set in the downstream direction from the pick-up head to avoid interference with the measurements. The body of the instrument could be moved vertically, and

during the tests the "foot" rested against the surface of the wing. The "foot" maintained a rigid connection between the wing and the body of the instrument and minimized errors in the relative position of the measuring head to the wing.

A screw jack was provided to change the vertical position of the central shaft in the body of the instrument, and their relative movement could be read from a dial-type displacement gauge mounted below the floor of the test section. Electrical connections were provided from the pick-up head to one side of a resistance gauge and from the copper tubes in the wing surface to the other side of the gauge. Boundary layer measurements were made at points where tubes were located in the surface of the wing, so that when the pick-up head was brought in contact with the surface of the wing an electrical circuit was completed, and this was registered on the resistance gauge. It was possible to determine the starting point for the distance measurements in this manner to a high degree of accuracy. With the pick-up head in contact with the wing, the dial gauge was set to a value of one-half the height of the tubes in the pick-up head (0.012 inch). This made it possible to read directly from the dial gauge the distance of the center of the tubes in the pick-up head from the surface of the wing.

The pick-up head of the instrument consisted of three flattened 1/32-inch (outside diameter) tubes which were attached together side by side in a plane parallel to the wing surface and with open ends of the tubes pointing upstream (Figure 4). The two outside tubes were about one tube diameter shorter than the center tube and were cut off at an angle of about 30 degrees to the axis of the tubes. This was done to provide lower total-pressure recovery for the side tubes when the pick-up

head was aligned with the flow, and thus improve the sensitivity of the instrument to yaw. The three tubes were led out through the central shaft to a manometer board beneath the test section. After setting the pick-up head a given distance from the surface of the wing the operator could rotate the instrument until the two side tubes registered the same pressure. The flow direction could then be read from a protractor which showed the angular position of the pick-up head with respect to the free-stream direction and the total pressure could be read from the center tube manometer indication.

An adjustment was provided so that the tubes of the pick-up head could be re-aligned with the surface of the wing when the angle of attack was changed or the position of the instrument on the wing was varied.

### III TESTS AND ANALYSIS OF THE DATA

#### Test Conditions and Configurations

Six different wing planforms were used; sweepback angles of 0, 20, 35, and 45 degrees were tested with an aspect ratio of 6, and with 35 degrees sweepback, aspect ratios of 4 and 8 were also tested. Measurements were made at many points on each planform, as determined by requirements for the establishment of spanwise and chordwise variations of the results and by the limitations of the instrumentation. Static-pressure measurements were made at 5, 10, 15, 20, 30, 40, 50, 60, 70 and 80 percent of the chord from the leading edge of the wing, and boundary layer surveys were made at 15, 40, 60 and 80 percent chord positions. The spanwise distribution of stations tested varied among the planforms and is shown in the presentation of many of the data.

The free-stream velocity was approximately 235 ft/sec for all the tests, resulting in a Reynolds number based on the normal flow of about  $7.5 \times 10^5 \cos \Lambda$ . The use of constant velocity rather than constant perpendicular flow Reynolds number was chosen to keep the Reynolds number as high as possible and to simplify the data reduction. The Mach number for the tests was about 0.2.

The boundary layer present on the wall of the test section where the wing was mounted is shown in Figure 5. The tunnel boundary layer bleed flow required to obtain the minimum boundary layer thickness where the wing was mounted was determined with the wing removed, and the bleed flow was set at this amount for all tests.

#### Test Procedure

With the model clamped in position for a particular planform, the testing procedure was as follows: The Scotch tape was removed at one spanwise

station and surface pressure distribution data were taken for the range of angles of attack covered in the tests. Boundary layer characteristics were then measured for each angle of attack to complete the tests for that spanwise station. Next, the static-pressure holes were covered and another set of holes was uncovered. The same testing procedure was then repeated for the new station, and so on until the complete planform had been covered.

The various data were taken visually by one person, who transmitted them by telephone to another who recorded the values and reduced some of the data. It was possible for the operator of the boundary layer instrument to select, by reference to the boundary layer total-pressure indication, more or less optimum height intervals for taking boundary layer data. This procedure minimized the number of points needed in a boundary layer traverse in order to determine the boundary layer profile.

#### Data Reduction

By operating the wind tunnel at constant dynamic pressure, it was possible to read the pressure data in coefficient form. The pressure coefficients were read from specially prepared scales on the manometer panels and were given in the form  $C_p = \frac{p_{\text{measured}} - p_o}{q_o}$ . For wing surface pressure distribution, the coefficients were plotted directly, and the pressures were extrapolated over the forward 5 percent and rear 20 percent of the chord where no measurements were taken, using theoretical pressure distribution as a guide in the extrapolation. The local lift coefficients were found by planimetry of the areas inside the pressure distribution plots.

Symbolically,

$$C_l = \int_0^1 (C_{pp} - C_{ps}) d(s/c).$$

Local lift coefficient was plotted against angle of attack and against the spanwise coordinate  $\frac{y}{b/2}$ , of the 25-percent-chord point of each pressure



measuring station to show the spanwise distribution of lift. The areas under the span-load curves were determined to find the total wing lift coefficients.

In order to compare the chordwise pressure distributions for various planforms and spanwise stations on the basis of the same local lift coefficient based on the normal flow, the pressure data were cross-plotted against angle of attack. The angle of attack corresponding to a given lift coefficient was determined from a plot relating these two variables. For a given  $C_l$  it was possible, then, to find  $C_l = C_{l_n} / \cos^2 \Lambda$ , and the corresponding angle of attack, and read the pressure distribution from the cross plot. These pressures were then resolved to find the pressure coefficient based on the normal flow,

$$C_{p_n} = C_p / \cos^2 \Lambda .$$

Total pressures in the boundary layer were also read directly in coefficient form,

$$C_{p_t} = \frac{p_t - p_o}{q_o}$$

The person recording the data was supplied with a plot of the incompressible boundary layer relation,

$$\frac{v_R}{V_R} = \sqrt{\frac{C_{p_t} - C_p}{1 - C_p}}$$

With  $C_p$  determined previously  $v_R/V_R$  could be read from the chart as the boundary layer total pressure data were taken at each point in a traverse. Using this procedure, the boundary layer total-pressure data were recorded as plots of resultant-velocity profiles  $v_R/V_R$  vs. the distance from the wing surface  $z$ , and the measured flow directions were recorded for each point in the profiles. Displacement thickness of the resultant boundary layer was determined to give an indication of the boundary layer growth

over the wing. The usual two-dimensional definition was applied to the resultant profile.

$$\delta_R^* = \int_0^{\delta} \left(1 - \frac{v_R}{V_R}\right) dz.$$

The boundary layer profiles were resolved to find the normal component of the flow field. The normal boundary layer velocity ratio  $v_n/V_n$  was calculated from the relation

$$\frac{v_n}{V_n} = \frac{V_R \cos(\Lambda + \phi)}{V_R \cos(\Lambda + \phi_S)}.$$

The displacement and momentum thicknesses of the normal boundary layer were found by planimetry of the areas defined by the velocity profiles, consistent with the thickness definitions,

$$\delta_n^* = \int_0^{\delta} \left(1 - \frac{v_n}{V_n}\right) dz \quad \text{and}$$

$$\theta_n = \int_0^{\delta} \left(\frac{v_n}{V_n} - \frac{v_n^2}{V_n^2}\right) dz.$$

The shape parameter for the perpendicular boundary layer was calculated from

$$H_n = \frac{\delta_n^*}{\theta_n},$$

and  $v_n/V_n$  was read from a large number of profiles at constant values of  $z/n$ . From this, a plot of  $v_n/V_n$  vs.  $H_n$  and  $z/n$  was made for comparison with two-dimensional generalizations of the same form.

IV EXPERIMENTAL RESULTSAccuracy and Applicability

The most severe limitations on the applicability of the results of the tests reported here were caused by the small scale of the model. The Reynolds number was only a small fraction of representative full-scale values, and the test results cannot be considered as representing accurately the phenomena for full-scale wings, but rather as showing general trends and possible generalizations. The use of roughness strips to fix boundary layer transition near the leading edge overcame the small-scale problem of shifting transition and made the results more consistent and more representative of full-scale conditions. However, the artificial disturbance created by the roughness strips caused an additional approximation to be made in the representation of the full-scale phenomena. The effects of the transition strips on the boundary layer profiles are shown in Figure 6. It will be noted that there appears a definite wake of the strip in the boundary layer profiles. The results for 12-degree angle of attack show the large effect of the transition strips on the separation. The strips are apparently acting as miniature vortex generators, mixing high-energy air with the air flowing near the surface and thus forestalling separation. The effect of the Scotch tape used to seal the holes in the surface pressure tubes is also shown in Figure 6. Although some differences appear between tests with tape and without, the boundary layer profiles do not seem to be greatly affected. The boundary layer results, particularly the velocity profile shapes, are somewhat depreciated in value by the effects of the roughness strip and tape. Because of the large effects of Reynolds number and the roughness strips on the boundary layer thickness, the magnitudes of thickness measured in the subject tests have no signifi-

cance in application to full-scale problems. However, the nature of the variation of boundary layer thickness over the wing is felt to be somewhat representative of full-scale variations.

No particular attention was devoted to obtaining extreme accuracies in the test measurements, because it was felt that the presence of serious limitations on scale did not justify great accuracy. Angle of attack setting was accurate to within about one-fourth of a degree; however, deflections of the model and flow asymmetries in the wind tunnel probably caused errors as high as a degree or more. Some small irregularities in the surface of the model were noted, but calibration tests at zero angle of attack showed their effect to be small. No correction for the effects of wind tunnel wall interference has been made, since sample calculations showed these effects to be small compared with the other approximations in the tests.

Most of the pressure measurements are probably accurate to within about 0.02 of the free-stream dynamic pressure, although a few of the data were considerably more in error due to leaks in the pressure leads. Flow direction was determined to within about 2 degrees except very near the wing surface, where the accuracy was rather poor due to the low velocities. For the boundary layer tests, distances from the wing surface were probably in error no more than about 0.01 inch.

The measurements made in the subject tests were checked for consistency by repeating parts of the tests after intervening model changes. The results of these repeatability tests are shown in Figure 7. Good agreement between the basic and check test data indicates that the measurements during the tests are probably quite consistent among the various measuring points and planforms tested.

### Surface Pressure Distribution and Lift

The wing surface pressure data are given in the form of chordwise-pressure-distribution plots on isometric drawings of the wing planforms in Figures 8 and 9. The effect of sweepback for an aspect ratio of six is shown in Figure 8 and the effect of aspect ratio for a sweepback of 35 degrees in Figure 9. The variations in sweepback and aspect ratio are both shown for the four angles of attack, 4, 8, 10 and 12 degrees, that were used in the tests.

It was not possible to measure pressures at the root and tip of the wing; however, pressures were measured within about a quarter chord of the wing ends. From the data obtained a slight amount of longitudinal shift in the pressure peaks can be noted for the wings with sweepback, but it appears that the effects of the tip and root on the pressure distribution decrease to a very small value in less than one-half the chord length from the wing ends.

For angles of attack of 4 and 8 degrees the pressure distributions appear quite regular outside of some scatter of the data for all the planforms except the 45-degree-swept back wing, where a slight disturbance of the regular pressure distribution appears (Figure 8). The disturbance appears to originate about one quarter of the semi-span from the root as a local decrease in the suction-surface pressure near the leading edge. The localized decrease in pressure is farther aft at the more outboard measuring stations and has disappeared on the outboard 20 percent of the semi-span, apparently having passed off the trailing edge.

For the higher angles of attack, 10 and 12 degrees, the pressure distributions become more irregular, especially for the higher sweepback angles. The type of pressure disturbance noted above is present in several cases at

the higher angles of attack, and in some cases there appear to be two separate disturbances. In some of the more extreme cases the disturbances give essentially constant pressure for a distance on the upper surface, and from this it is supposed that they are associated with localized separation. Most of the boundary layer profiles have reversals in the velocity variation with distance from the wing surface at points of severe pressure disturbance, and some of the profiles of the normal flow show separation. It is thought that this localized, laminar "bubble" type of separation leads to the formation of a continuous vortex streak, which streams outboard and aft, accounting for the noted variation in location of the disturbance. The separation streak has an increasing effect on the pressure distribution as the sweepback is increased, as can be seen from Figure 8. The higher-aspect-ratio planforms also seem to be slightly more affected than the lower aspect ratios.

It can be noted that at 12 degrees angle of attack at a point about one-third of the semi-span inboard from the tip on the 35-degree-sweepback planforms of aspect ratio 6 and 8 there is an indication of separation over the entire chord length. However, there is some pressure recovery, indicating a tendency toward re-attachment of the flow. A spreading-out of the separation streak over a larger chordwise distance can be noted as the distance from the origin of the streak is increased. It may be that the complete separation noted above is the result of this spreading-out process.

These tests do not show enough detail to describe the type of separation noted adequately. It does appear from the test results, however, that laminar "bubble" type of separation can lead to the formation of a separation vortex streak which streams outboard and aft and has the same effect in locally decreasing the surface pressure as a similarly situated ridge on

the wing surface. It should be noted that it is not certain that the boundary layer is laminar at the origin of the separation streak and that it is definitely turbulent over the greater part of the length of the streak. Thus it appears that localized separation with subsequent re-attachment of the flow can occur with a turbulent boundary layer, in the case of swept back wings, at least for the low Reynolds numbers of the present tests.

The variation in local lift coefficient with angle of attack, as determined from the surface pressure measurements, is presented in Figure 10 for several spanwise stations for each of the planforms tested. For zero and 20 degrees sweepback the local lift curves are of the usual, two-dimensional form with constant slope at low angles and decreasing slope at higher angles as the stall is approached. However, for the higher sweepback angles some of the local lift curves show an increase in slope at about 10 degrees angle of attack. This increase in slope is caused by the local separation phenomenon that is discussed above. The separation of the perpendicular flow causes an effective increase in the thickness and camber of the wing. It can be noted that the local lift curves showing the increase in slope at high angles of attack are for adjacent spanwise measuring stations in each planform case. This lends further credence to the idea that a continuous vortex separation streak is formed, causing the unusual variation in pressure distribution noted above.

The spanwise distribution of lift for the various planforms tested is presented in Figure 11 with a comparison of the distribution found for the same total lift coefficient using the Weissinger theory. Large discrepancies between the test and theoretical results are noted, particularly for the higher sweepback angles. The outboard shift of the center of pressure

with increasing sweepback is much less pronounced than that predicted by theory. For zero sweepback the lift near the tip is higher than predicted and for other sweep angles it is lower except very near the tip. The similarity in shape of the span-load curves for various angles of attack is seen to hold very well for angles of 4 and 8 degrees for all planforms. For the higher angles of attack, however, there are some pronounced changes in the shape of the span-load curves, especially for the higher sweepback angles. For an aspect ratio of 6 the change in shape is very pronounced between 10 and 12 degrees angle of attack for a sweepback angle of 35 degrees and is less pronounced, yet definitely present for 45 degrees sweepback between 8 and 10 degrees angle of attack. In these cases stall at the tips is evident with regions of high local lift in the center of the semi-span, which can be seen from the surface pressure distribution plots to be caused by the localized separation phenomenon.

The total lift for the various wing planforms as found from integration of the span-load curves is presented in Figure 12 as a function of angle of attack. The curves for aspect ratio 6 for 35 and 45 degrees sweepback and the aspect ratio 4, 35 degree sweepback curves exhibit an increase in slope between 10 and 12 degrees due to the localized separation. It can be seen that the slope for low angles of attack increases with aspect ratio as predicted by the Prandtl wing theory in changing from 4 to 6 aspect ratio at 35 degrees sweepback. However, very little change in lift-curve slope is indicated for a further increase in aspect ratio to 8. The reason for this is not apparent. The simple sweep theory for infinite span predicts a variation in lift-curve slope with sweepback as follows:

$$\left. \frac{dC_L}{d\alpha} \right|_{\Lambda} = \left. \frac{dC_L}{d\alpha} \right|_{\Lambda=0} \cos \Lambda$$



Reducing the slope of the various planforms of aspect ratio 6 to zero sweepback using this formula, the values presented in the table below are obtained.

$\Lambda$ (degrees)	$\cos \Lambda$	$\frac{dC_L}{d\alpha}$ (per degree)	$\frac{dC_L}{d\alpha} / \cos \Lambda$
0	1.0	.0675	.0675
20	.940	.0638	.0679
35	.819	.0550	.0672
45	.707	.0498	.0704

It appears that the simple sweep theory works quite well in predicting the variation in total-lift-curve slope with sweepback, particularly for sweepback angles up to 35 degrees. This agrees with the results of previous experiments (cf. Ref. 2). The increase in lift-curve slope reduced to zero sweepback for the 45-degree planform is probably due to the effect of the root and the tip tending to make part of the wing act as if it were not swept as much.

In Figure 13 the pressure distribution based on the normal flow is compared for the various sweepback angles at an aspect ratio of 6 and for several spanwise stations to indicate the validity of the extended simple sweep theory in predicting pressure distribution. It can be seen that the variation with sweepback is greatest near the root and the tips, as would be expected due to the longitudinal shift in pressure pattern at those locations. For the mid-semi-span station,  $2y/b \approx .45$ , the agreement among the various sweepback angles is good for the low-lift case,  $C_l / \cos^2 \Lambda = 0.4$ , but this agreement deteriorates as the lift is increased. No systematic variation with sweepback is noted in this generalization except near the root and tip, where the longitudinal shift in pressure pattern can be seen to a certain extent. Some of the variation in resolved pressure distributions with sweepback is probably caused by unavoidable inconsistencies in

extrapolation of the measured pressure data over the forward 5 percent and aft 20 percent of the chord.

#### Boundary Layer Thickness and Flow Direction Near Wing Surface

The displacement thickness of the resultant boundary layer flow is presented in Figures 14 through 17 in the form of contour plots on drawings of the various wing planforms. Arrows indicating the flow direction at the nearest point to the surface where measurements were taken (0.012 inches from the wing surface to the center of the pick-up tubes) are also included. The contours and flow direction arrows are shown only on those portions of the wing where measurements were taken, and this accounts for the blank spaces near the root and tip ends of the wings.

In several cases a maximum boundary layer thickness was reached about 20 percent of the chord from the leading edge followed by a decrease in the thickness and finally an increase again. It is not apparent what caused such a variation, but it is felt that the fact that it occurred in several different cases indicates that such a phenomenon actually can exist on a wing and was not caused in this case by errors in measurement or imperfections in the wing surface. No systematic variation of the peaking of the boundary layer thickness is apparent.

The regions in which the boundary layer measurements showed reversals in the variation of resultant velocity with distance from the wing surface are indicated in Figures 14 through 17 as regions of separated flow. This is not, of course, a rigorous definition; however, it was found that in such regions the boundary layer thickness behaved in an erratic manner. Therefore, it was felt that this criterion for separation described the onset of disturbances leading to stall as well as or better than other possible criteria.

The effect of outflow in the boundary layer on the swept back planforms

can be noted especially for the higher angles of attack, where the boundary layer thickness increases sharply toward the outboard trailing edge. It is also interesting to note the relation between the flow direction and the rate of increase of boundary layer thickness, which relation shows a decided increase in the out-flow in the regions where the thickness is increasing rapidly. Comparing the regions of separated flow with the surface pressure disturbances of Figures 8 and 9 shows some correlation between the occurrence of the two phenomena. However, the correlation is not complete, indicating that it is possible to have localized pressure disturbances without reversals in the resultant boundary layer profiles and vice versa.

#### Generalization of the Normal Component of Boundary Layer Flow

In order to check the concept that the family of profile shapes assumed by the normal component of boundary layer flow is independent of sweepback, the shapes of a large number of boundary layer profiles for each sweepback for an aspect ratio of 6 are presented in Figures 18 through 21 in the form of plots of the boundary layer velocity ratio  $v_n/V_n$  vs. the shape parameter  $H_n$  for constant values of  $z/\theta_n$ . Curves have been faired through the data points, which are quite badly scattered. The generalizations of shape thus obtained are plotted in Figure 22 in the form of symbols spaced at intervals and representing the faired lines for the various sweepback angles of Figures 18 through 21. The generalizations of boundary layer profile shape found previously for unswept bodies are shown for comparison. There appears no systematic effect of sweepback on the generalization and the agreement with the previous generalizations for no sweepback is good, particularly with that of Reference 10.

## V CONCLUSIONS

Because of the low Reynolds number and other limitations of the tests reported here it is not possible to draw conclusions on a quantitative basis for application to the design of full-scale airplanes. However, the following items, which may be applicable at full scale on a qualitative basis, can be concluded from these tests.

1. Localized regions of separation followed by re-attachment of the flow can occur at angles of attack somewhat below the stall on swept back wings. The region of separation starts near the leading edge and runs outboard and aft in a continuous vortex streak. The separation leads to a localized increase in lift similar to the action of a smooth bump on the wing surface.

2. Considerable discrepancy can exist between the spanwise distribution of lift as obtained by test and as predicted by the Weissinger theory at lift coefficients somewhat below the stall, especially in cases where separation streaks are present.

3. The generalization of chordwise pressure distribution for various sweepback angles on the basis of the local lift coefficient and the normal component of flow is fairly accurate at low and moderate lift coefficients, except in the vicinity of the root and tip of the wing, where longitudinal shifts in the pressure patterns cause appreciable error. The effects of the root and tip on the pressure patterns have decreased to very small amounts by one-half chord distance from either root or tip.

4. Surface pressure distribution, boundary layer thickness and flow direction near the wing surface are related in a complex manner. No attempt has been made here to describe the relation among these factors. Solution of their interaction effects will probably require solution of

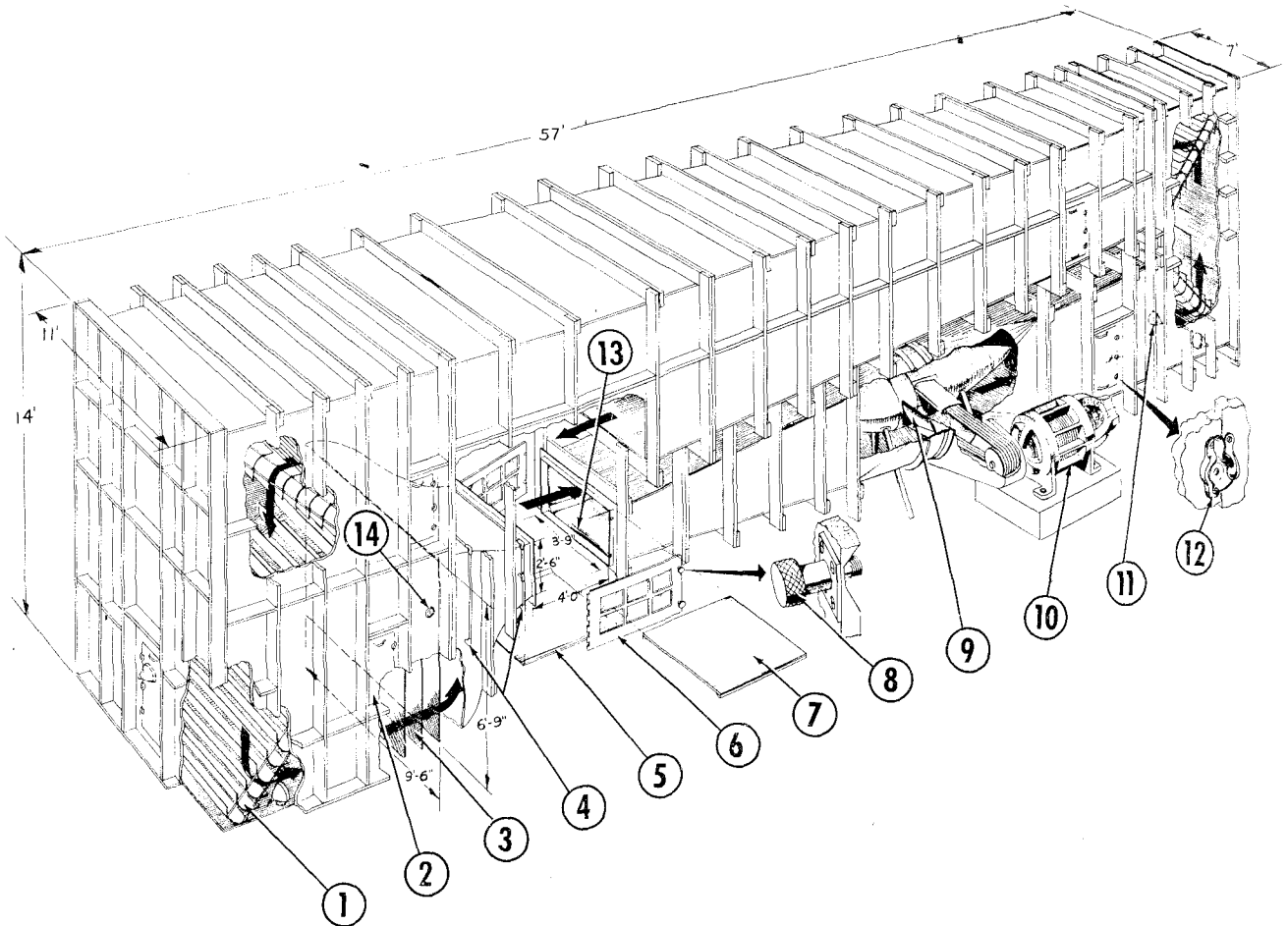
the individual components, such as the causes and effects of the separation streak, effects of pressure gradients on the boundary layer of swept back wings, etc.

5. The normal component of turbulent boundary layer flow on a swept back wing assumes a family of velocity profile shapes that can be described by one parameter. This generalization is independent of sweepback angle, and the family of boundary layer profile shapes found by earlier research on unswept bodies agrees well with that found from the tests reported here. If a generalization of the effect of pressure gradients on the normal component of boundary layer flow can be established for swept back wings, the shape generalization can be used in connection with the pressure gradient effect to predict quantitatively some of the boundary layer growth phenomena on swept back wings.

## VI REFERENCES

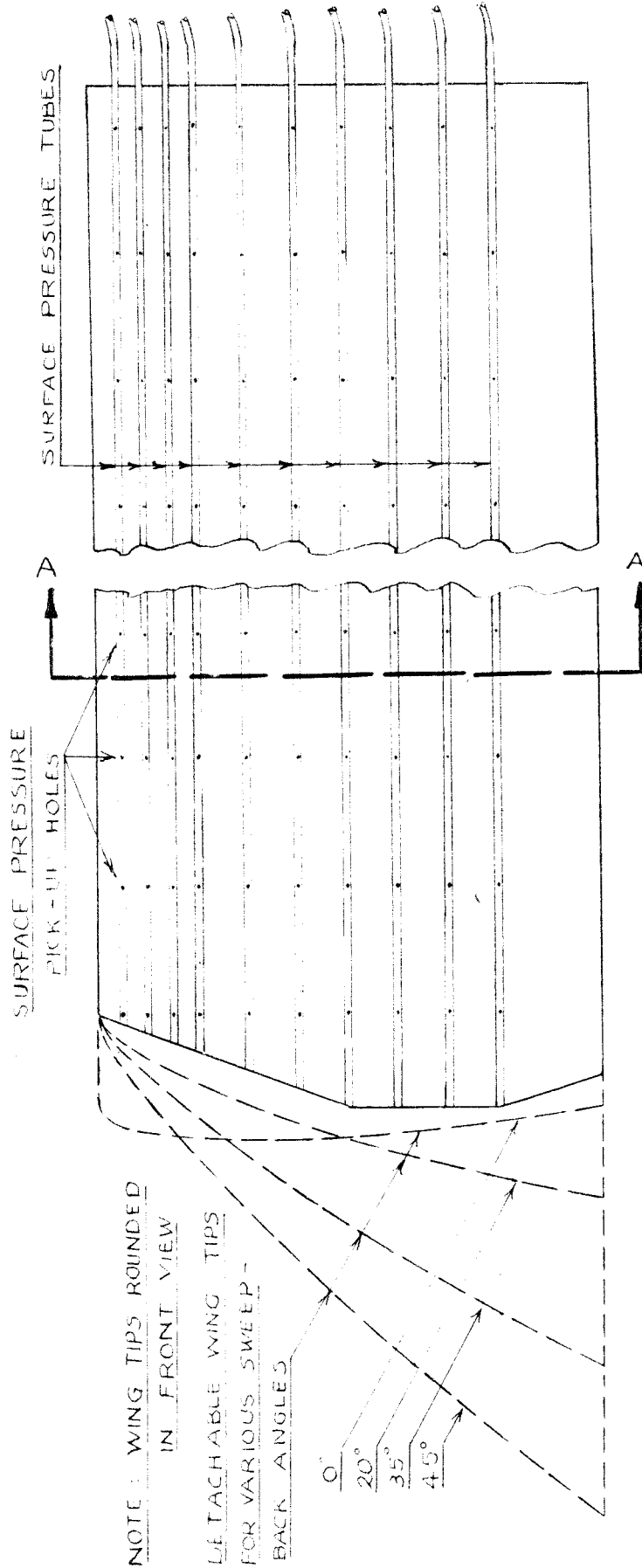
1. Shortal, Joseph A. and Maggin, Bernard: Effect of Sweepback and Aspect Ratio on Longitudinal Stability Characteristics of Wings at Low Speeds. NACA TN 1093, July 1946.
2. Holme, O.: Comparative Wind Tunnel Tests of a Swept Back and a Straight Wing Having Equal Aspect Ratios. The Aeronautical Research Institute of Sweden, Report No. 31, 1950.
3. Prandtl, L.: On Boundary Layers in Three-Dimensional Flow. M.A.P. Volkenrode MAP -VG 84, (British Reports and Translations No. 64), May 1, 1946.
4. Sears, W. R.: The Boundary Layer of Yawed Cylinders. Journal of the Aeronautical Sciences, Vol. 15, No. 1, p. 49, January 1948.
5. Wild, J. M.: The Boundary Layer of Yawed Infinite Wings. Journal of the Aeronautical Sciences, Vol. 16, No. 1, p. 41, January 1949.
6. Jones, Robert T.: Effects of Sweepback on Boundary Layer and Separation. NACA TN 1402, July 1947.
7. Bursnall, William J. and Loftin, Laurence K., Jr.: Experimental Investigation of the Pressure Distribution About a Yawed Cylinder in the Critical Reynolds Number Range. NACA TN 2463, September 1951.
8. Altman, John M. and Hayter, Nora-Lee F.: A Comparison of the Turbulent Boundary-Layer Growth on an Unswept and a Swept Wing. NACA TN 2500, September 1951.
9. von Doenhoff, Albert E. and Tetervin, Neal: Determination of General Relations for the Behavior of Turbulent Boundary Layers. NACA report No. 772, 1943.
10. Schubauer, G. B. and Klebanoff, P. S.: Investigation of Separation of the Turbulent Boundary Layer. NACA TN 2133, August 1950.
11. Kuethe, A. M., McKee, P. B. and Curry, W. H.: Measurements in the Boundary Layer of a Yawed Wing. NACA TN 1946, September 1949.
12. Burshall, William J. and Loftin, Laurence K., Jr.: Experimental Investigation of Localized Regions of Laminar-Boundary-Layer Separation. NACA TN 2338, April 1951.

## DOUGLAS EL SEGUNDO WIND TUNNEL



- ① VANES
- ② ACCESS DOOR
- ③ SCREENS (18 MESH COPPER WIRE DIA. .011)
- ④ PIEZOMETER RINGS
- ⑤ TEST SECTION BOTTOM PANEL
- ⑥ TEST SECTION DOORS
- ⑦ TEST SECTION TOP PANEL
- ⑧ DOOR CLOSING KNOB
- ⑨ FAN (4 BLADES)
- ⑩ ELECTRIC MOTOR (100 H.P.)
- ⑪ INSIDE LIGHTS
- ⑫ TYPICAL ACCESS DOOR LATCH
- ⑬ ATMOSPHERIC PRESSURE VENTS (BOTTOM AND SIDES ONLY)
- ⑭ THERMOMETER

# MODEL WING



NOTE: WING TIPS ROUNDED IN FRONT VIEW

DETACHABLE WING TIPS FOR VARIOUS SWEEP-  
BACK ANGLES

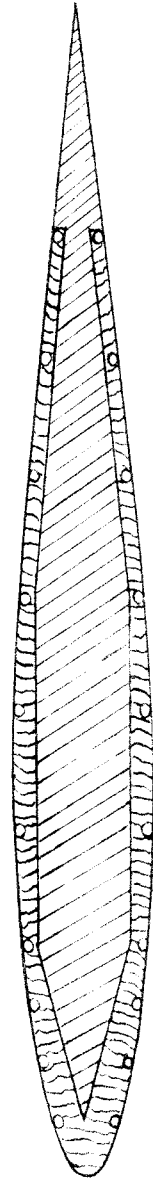
0°  
20°  
35°  
45°

MAHOGANY

STEEL



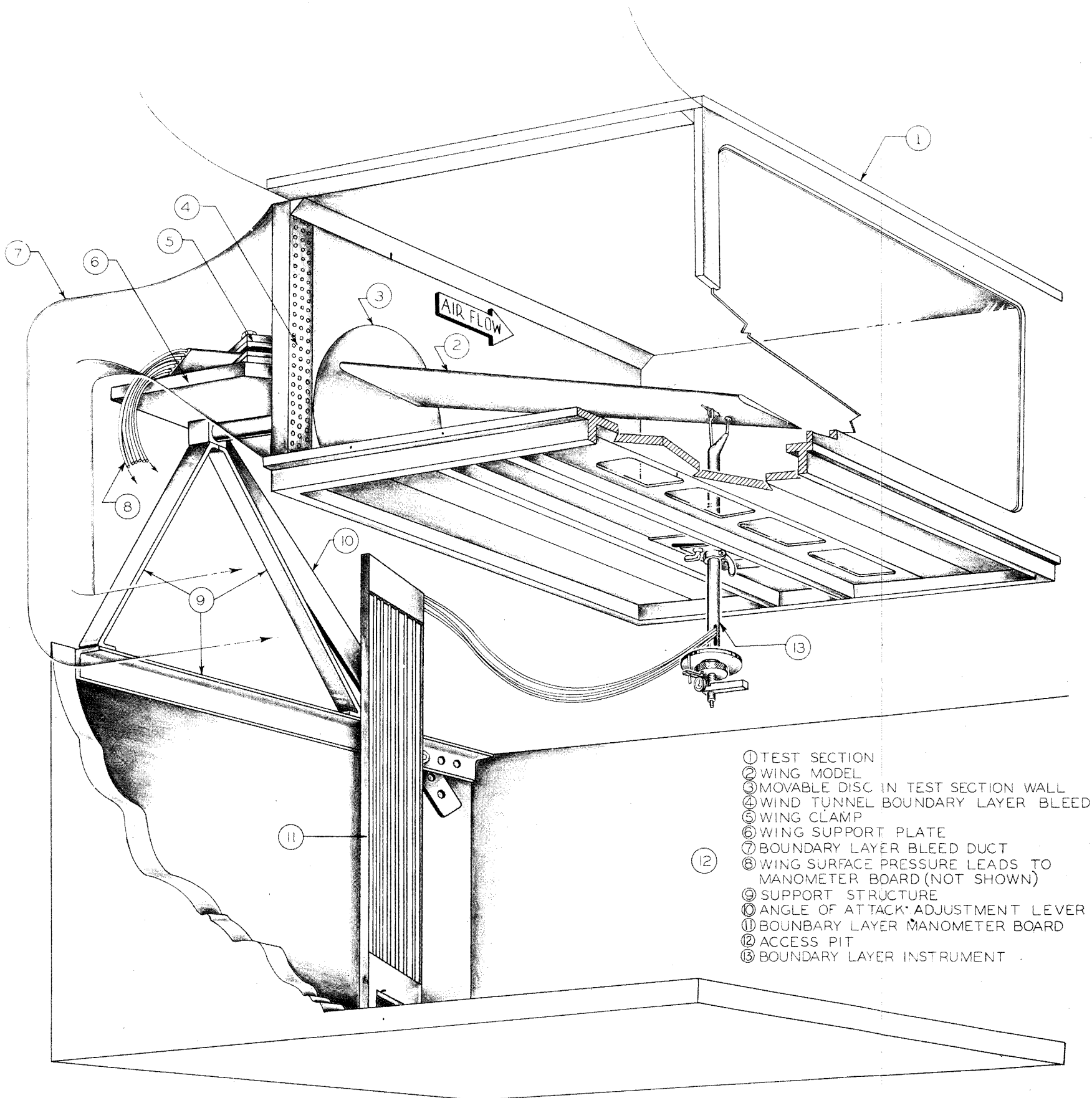
PRESSURE TUBES



SECTION A-A

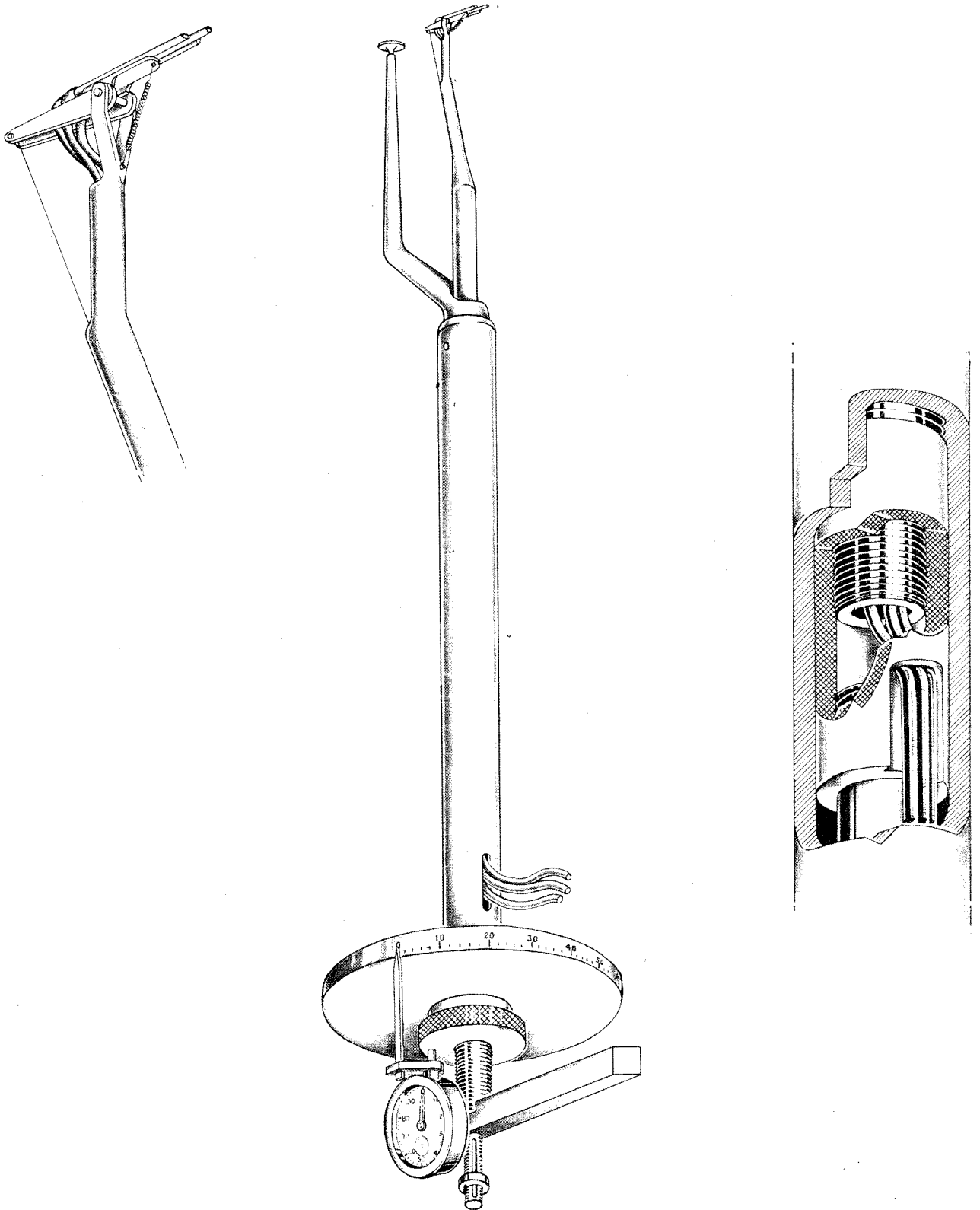


## TEST INSTALLATION



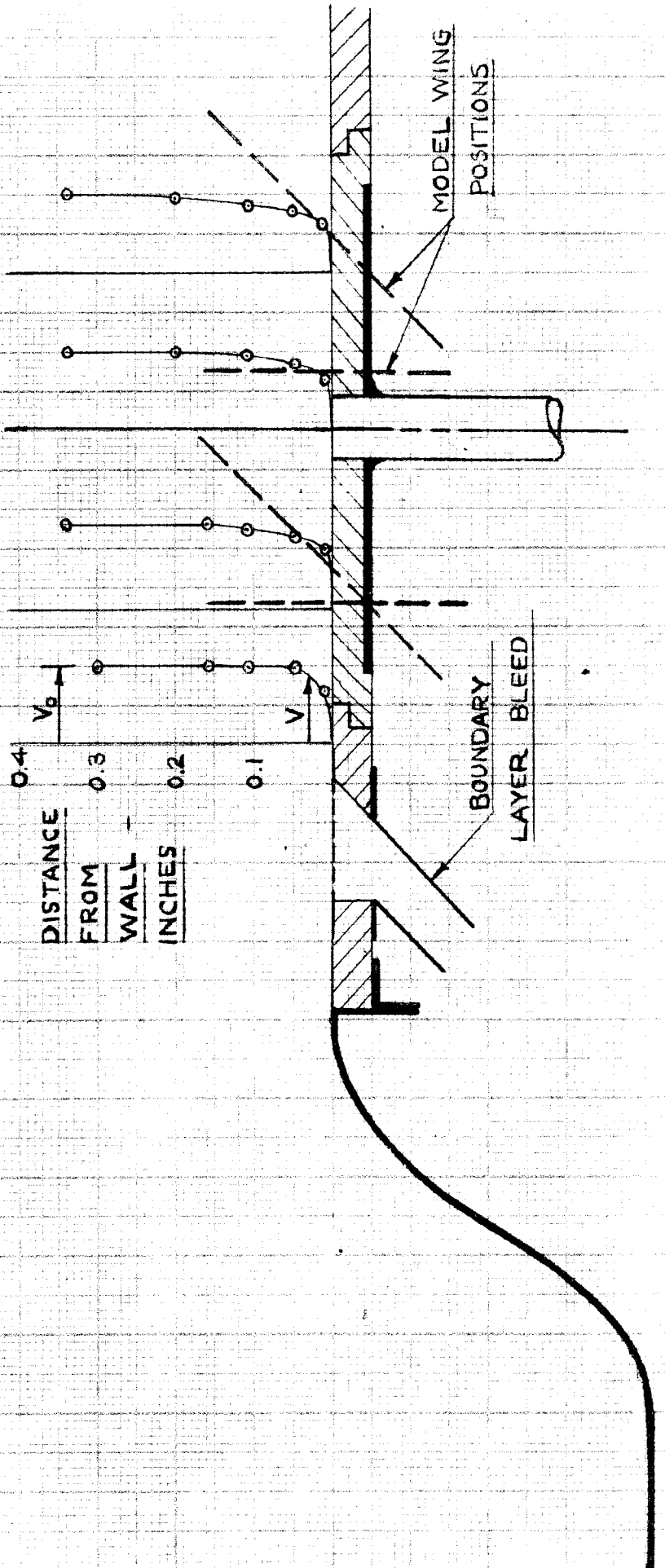
- ① TEST SECTION  
 ② WING MODEL  
 ③ MOVABLE DISC IN TEST SECTION WALL  
 ④ WIND TUNNEL BOUNDARY LAYER BLEED  
 ⑤ WING CLAMP  
 ⑥ WING SUPPORT PLATE  
 ⑦ BOUNDARY LAYER BLEED DUCT  
 ⑧ WING SURFACE PRESSURE LEADS TO MANOMETER BOARD (NOT SHOWN)  
 ⑨ SUPPORT STRUCTURE  
 ⑩ ANGLE OF ATTACK ADJUSTMENT LEVER  
 ⑪ BOUNDARY LAYER MANOMETER BOARD  
 ⑫ ACCESS PIT  
 ⑬ BOUNDARY LAYER INSTRUMENT

# BOUNDARY LAYER INSTRUMENT



# BOUNDARY LAYER VELOCITY PROFILES ON WIND TUNNEL WALL

$V_0$

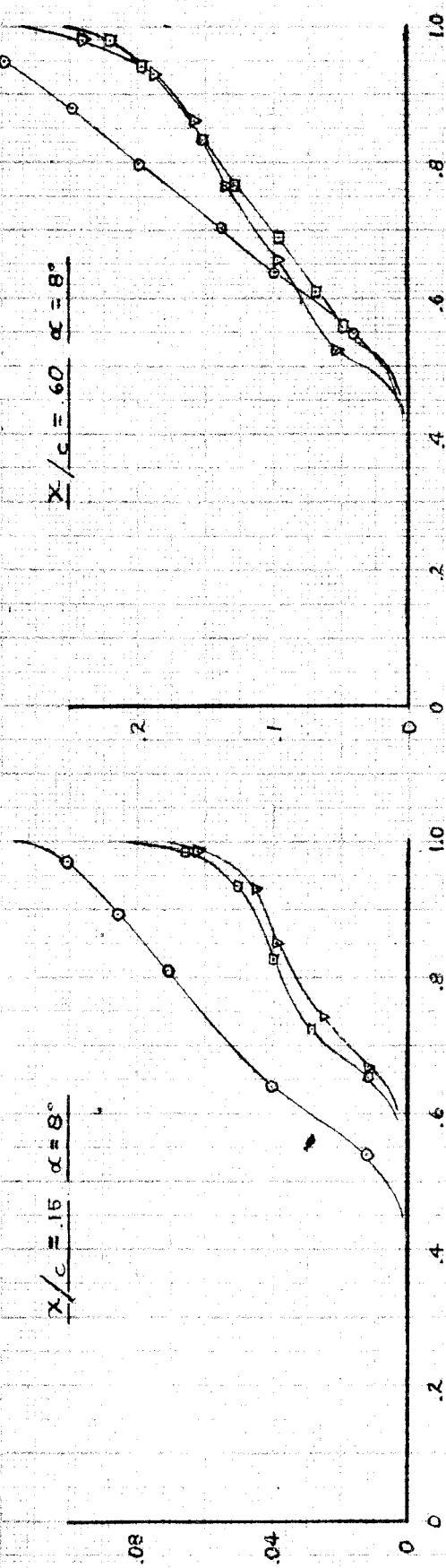



EFFECT OF TAPE AND TRANSITION STRIP SIZE  
ON BOUNDARY LAYER PROFILES

$\Lambda = 35^\circ$   $AR = 6$   $S = 5$

$x/c = .15$   $\alpha = 8^\circ$

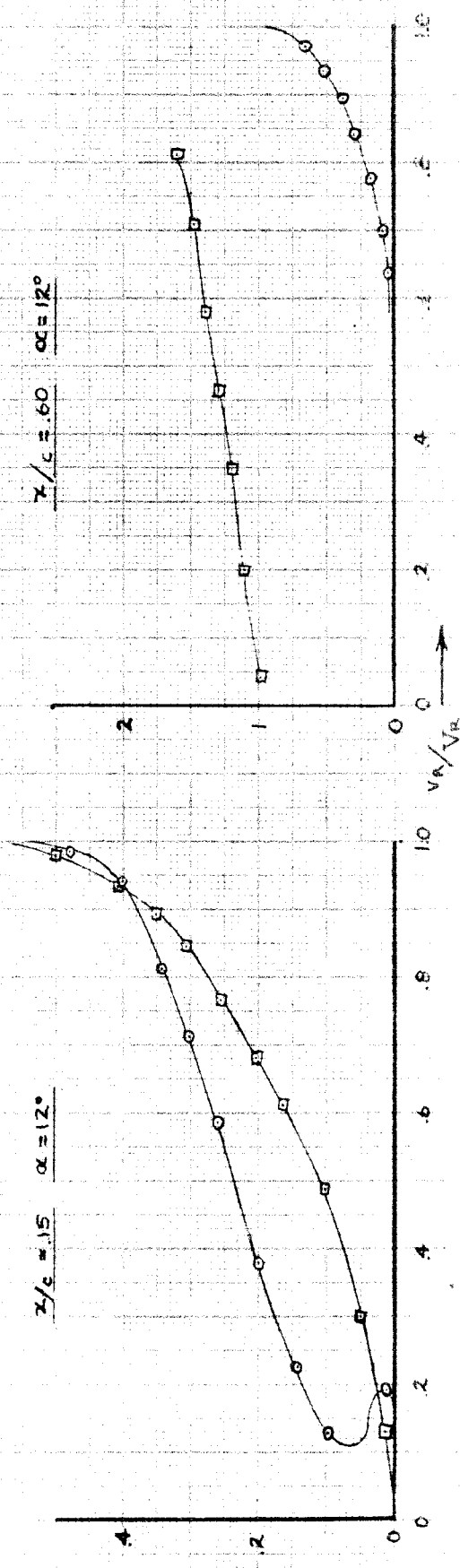
$x/c = .60$   $\alpha = 8^\circ$



○ LARGE TRANSITION STRIP - TAPE ON  
□ SMALL TRANSITION STRIP - TAPE ON  
▽ SMALL TRANSITION STRIP - TAPE OFF

$x/c = .15$   $\alpha = 12^\circ$

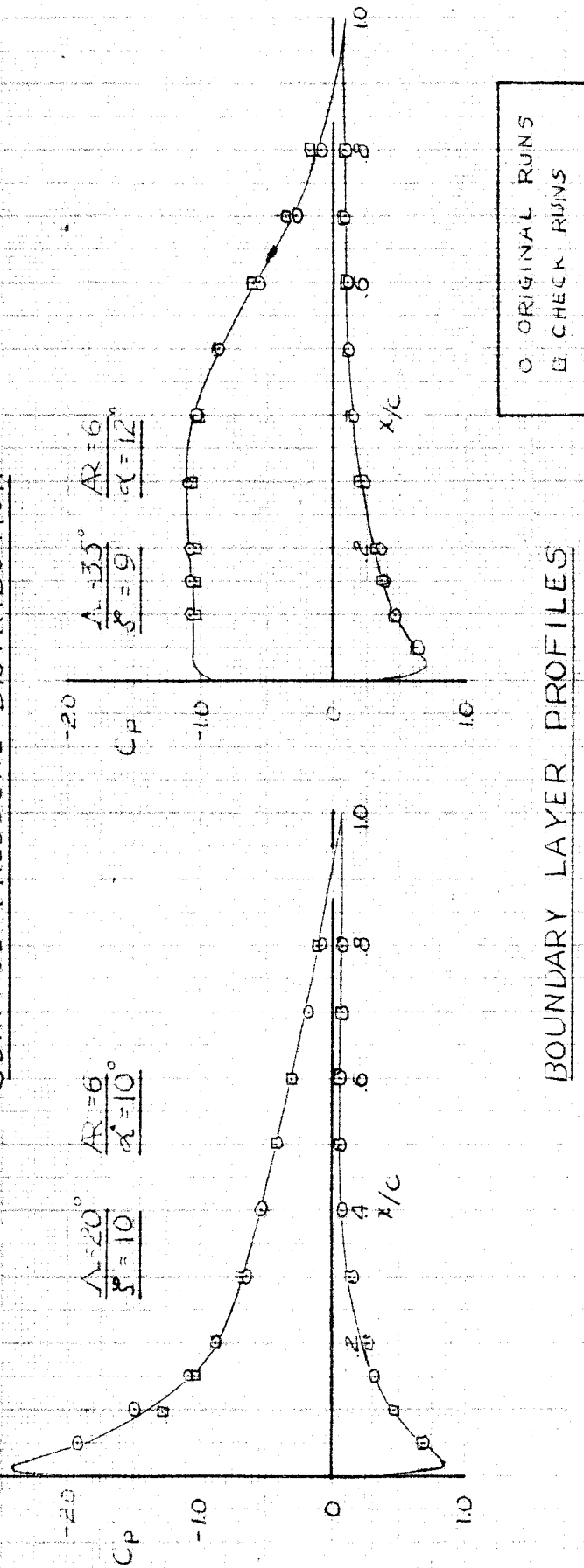
$x/c = .60$   $\alpha = 12^\circ$



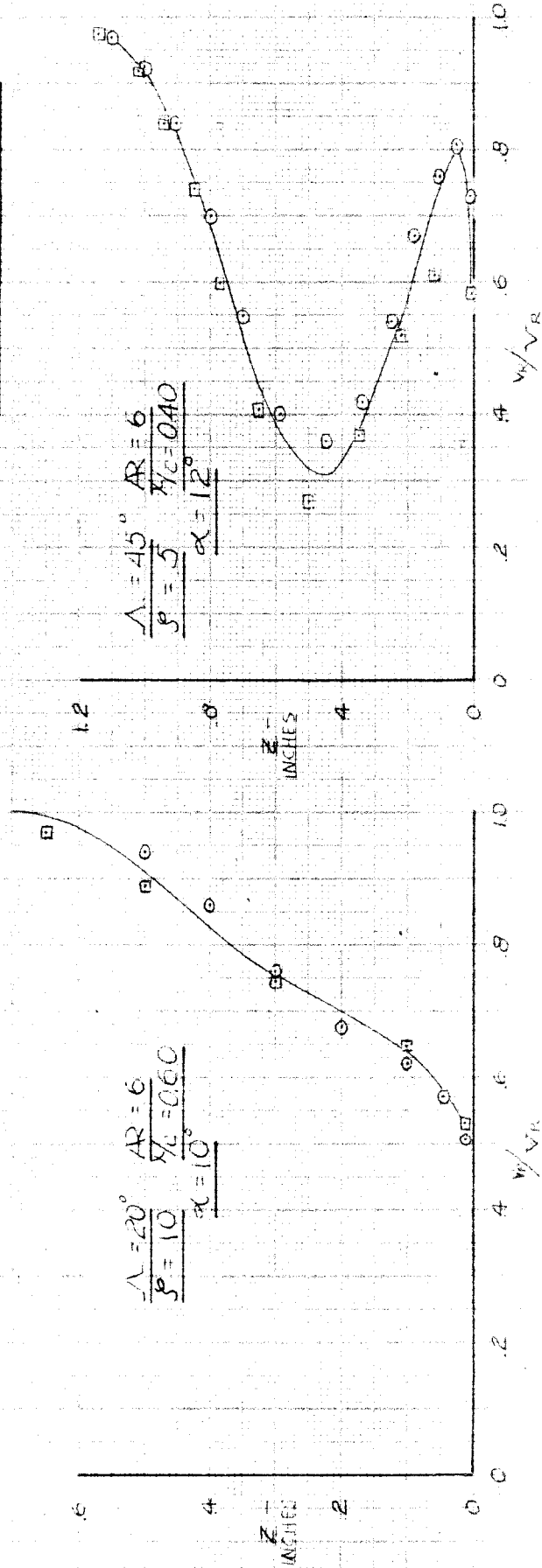
z - INCHES

REPEATABILITY OF DATA

SURFACE PRESSURE DISTRIBUTION



BOUNDARY LAYER PROFILES



# EFFECT OF SWEEPBACK AND ANGLE OF ATTACK ON SURFACE PRESSURE DISTRIBUTION

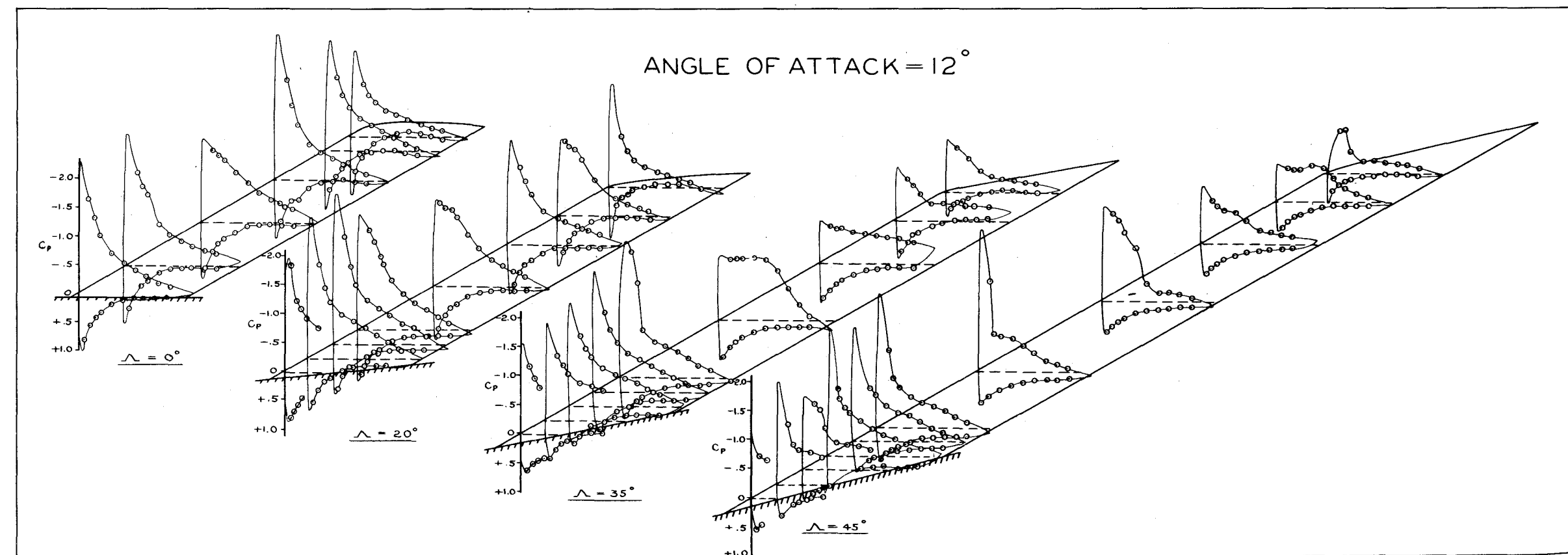
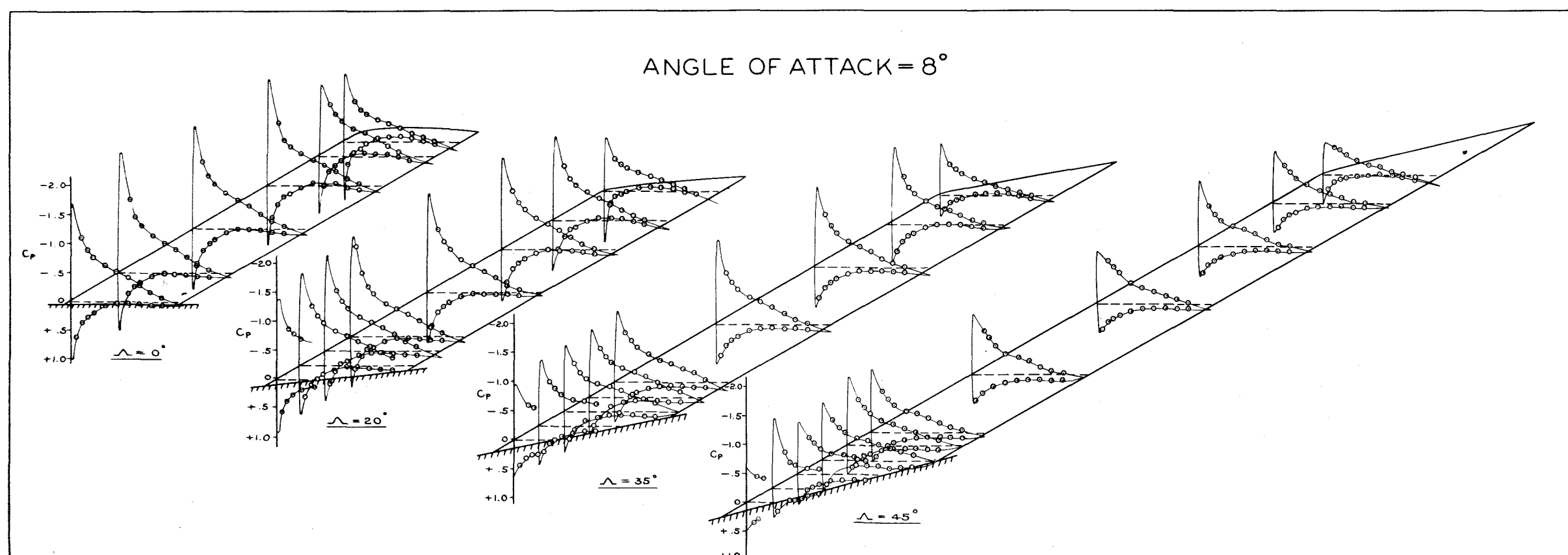
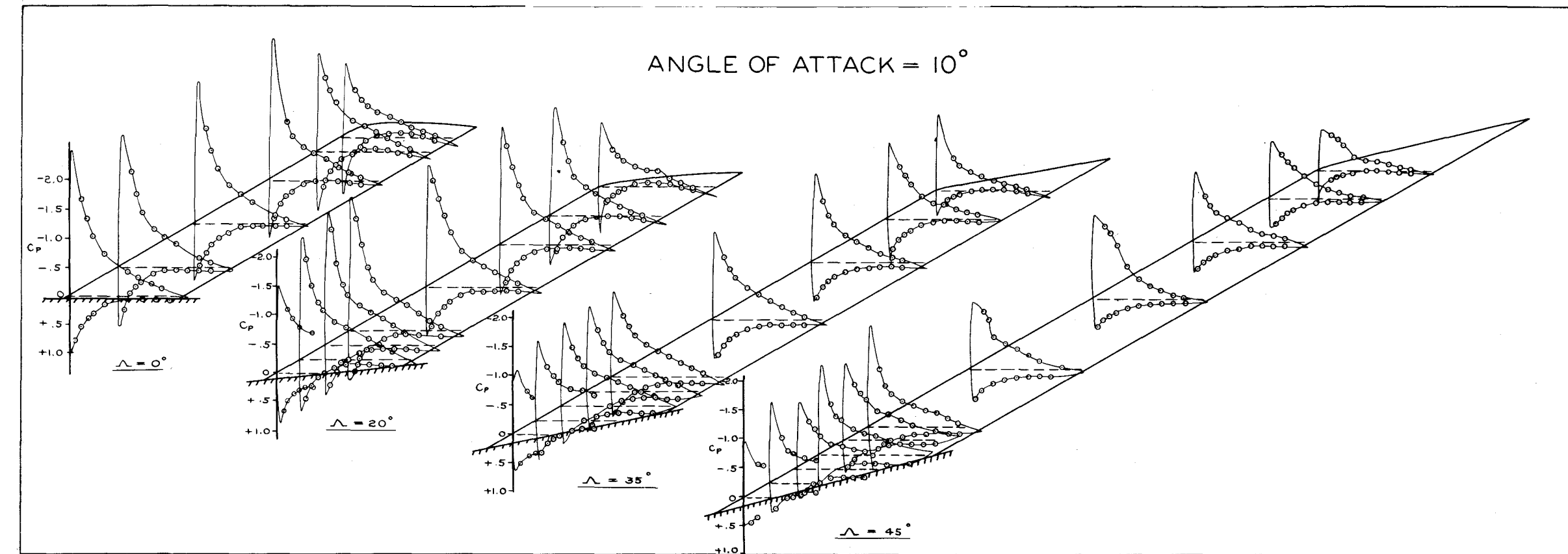
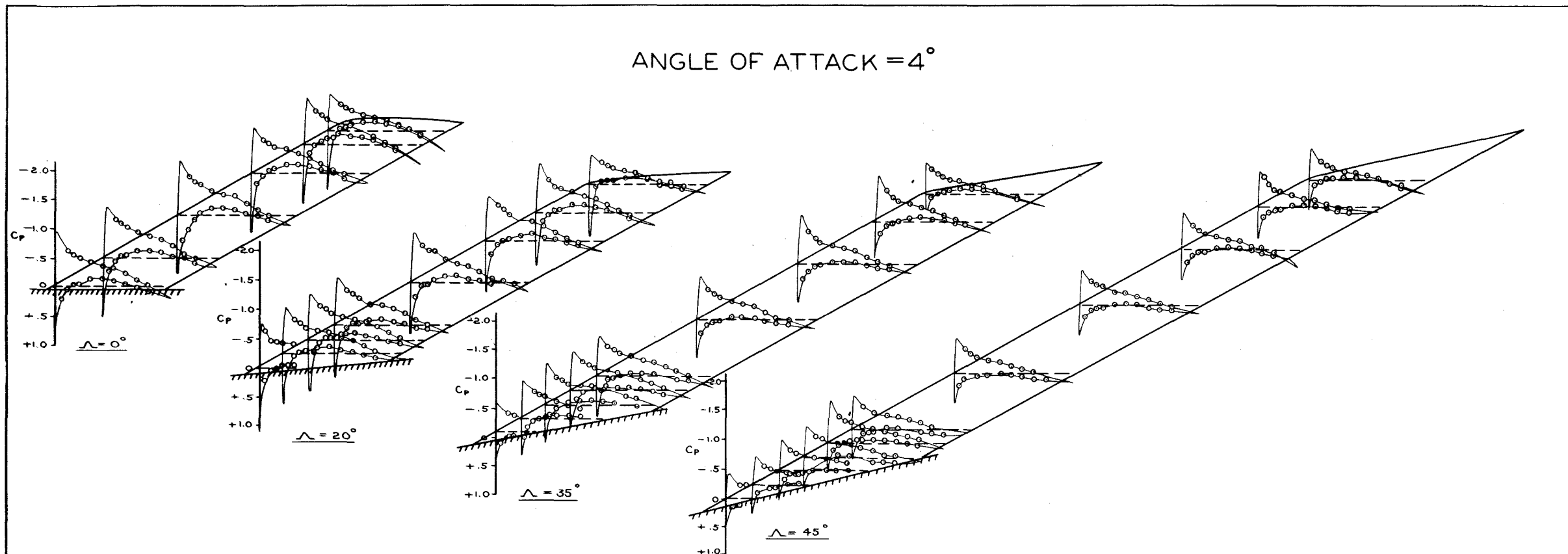
— ASPECT RATIO = 6

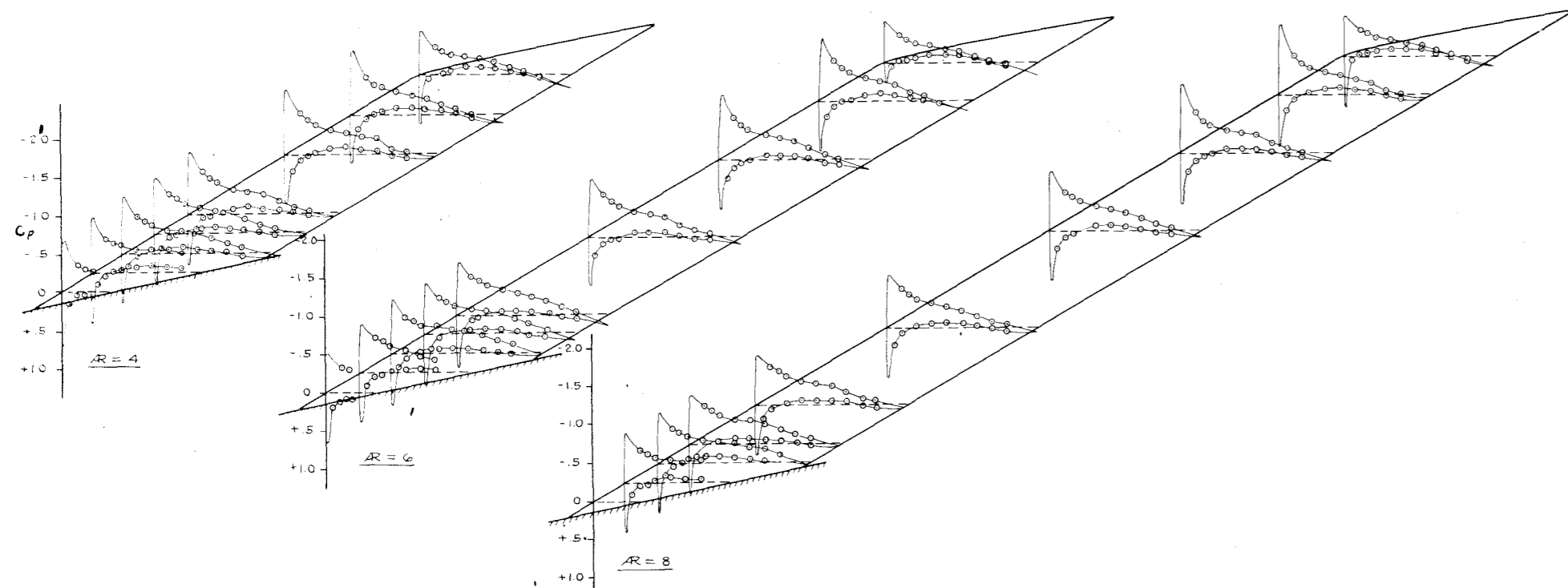
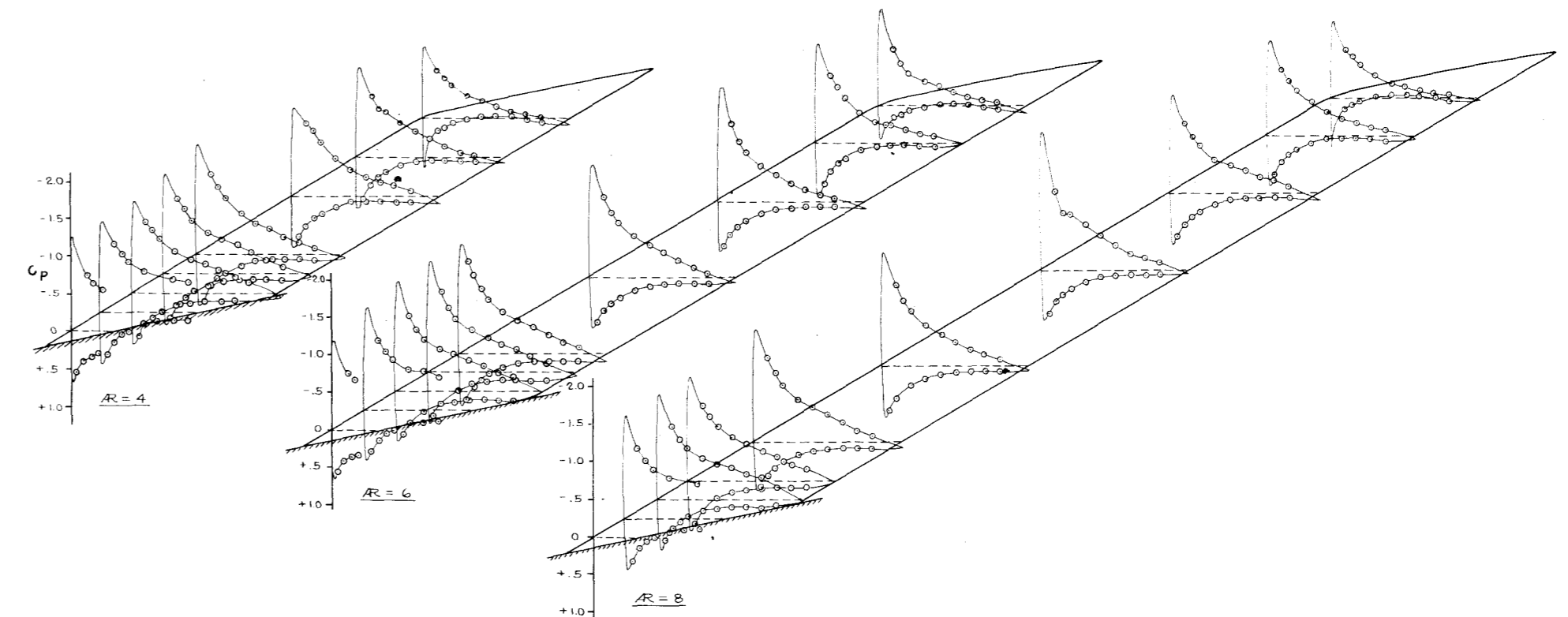
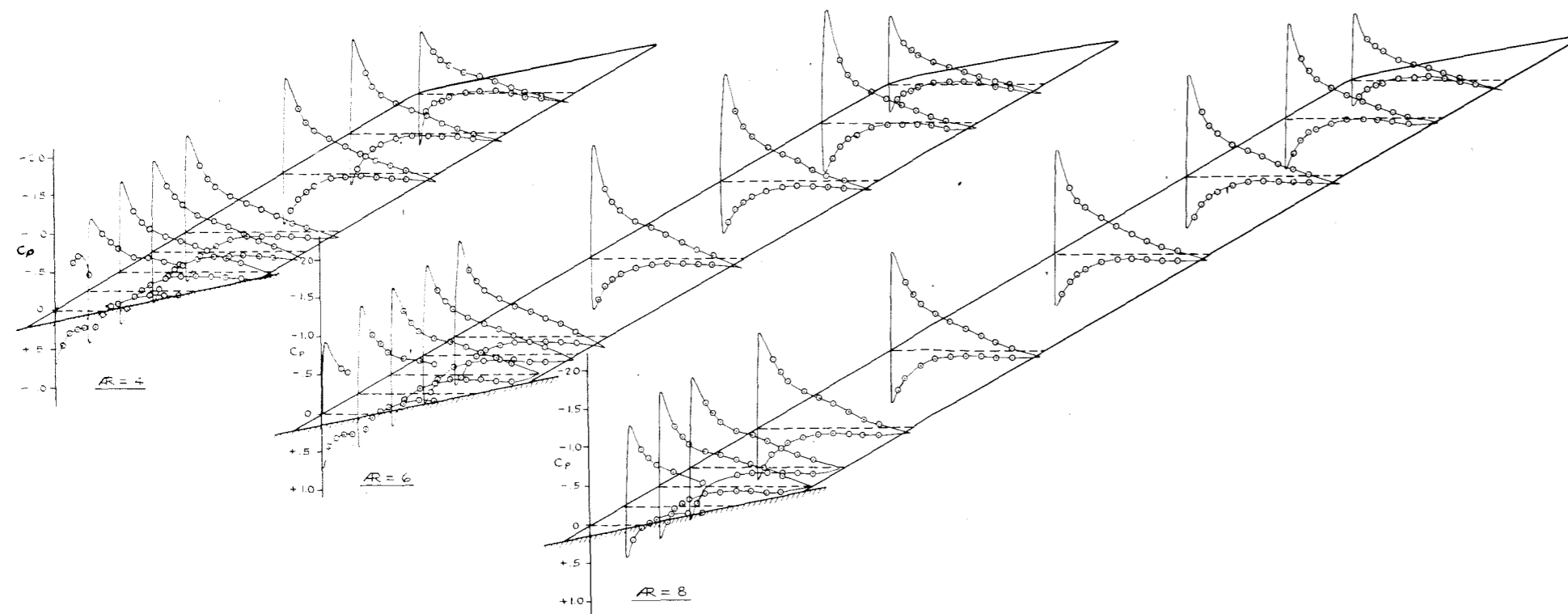
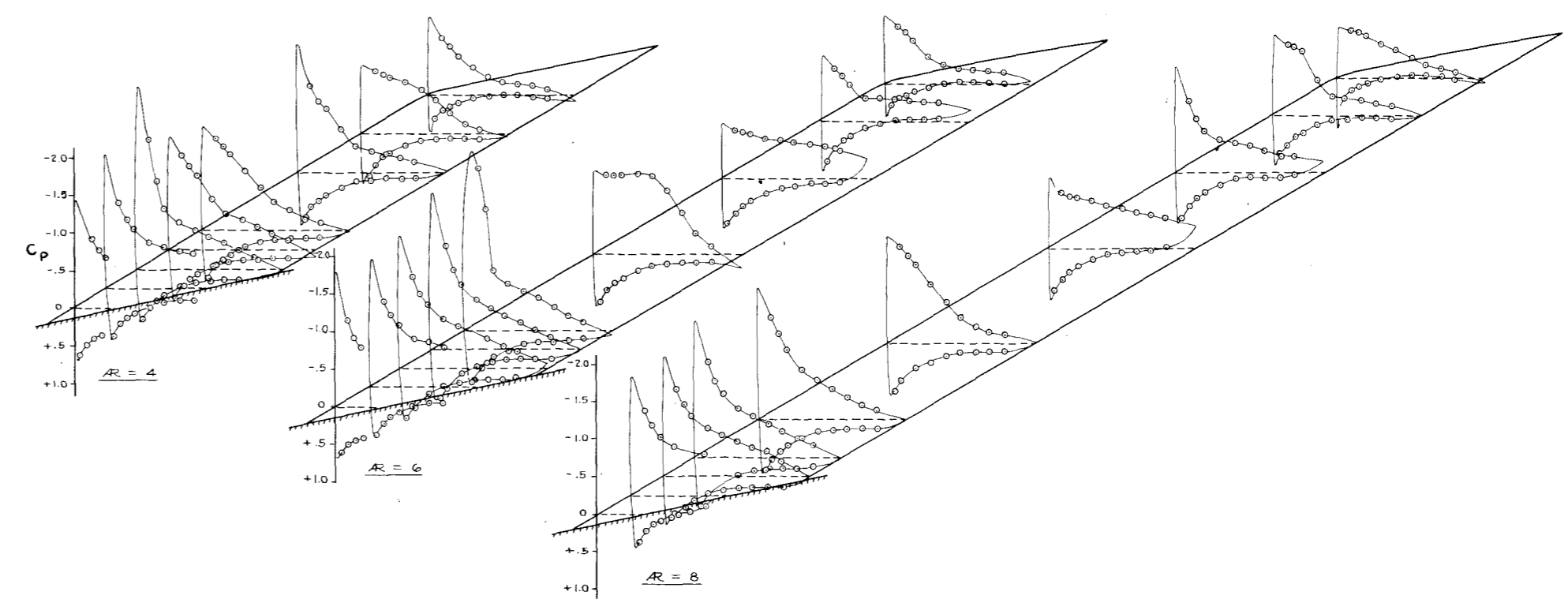
ANGLE OF ATTACK = 4°

ANGLE OF ATTACK = 10°

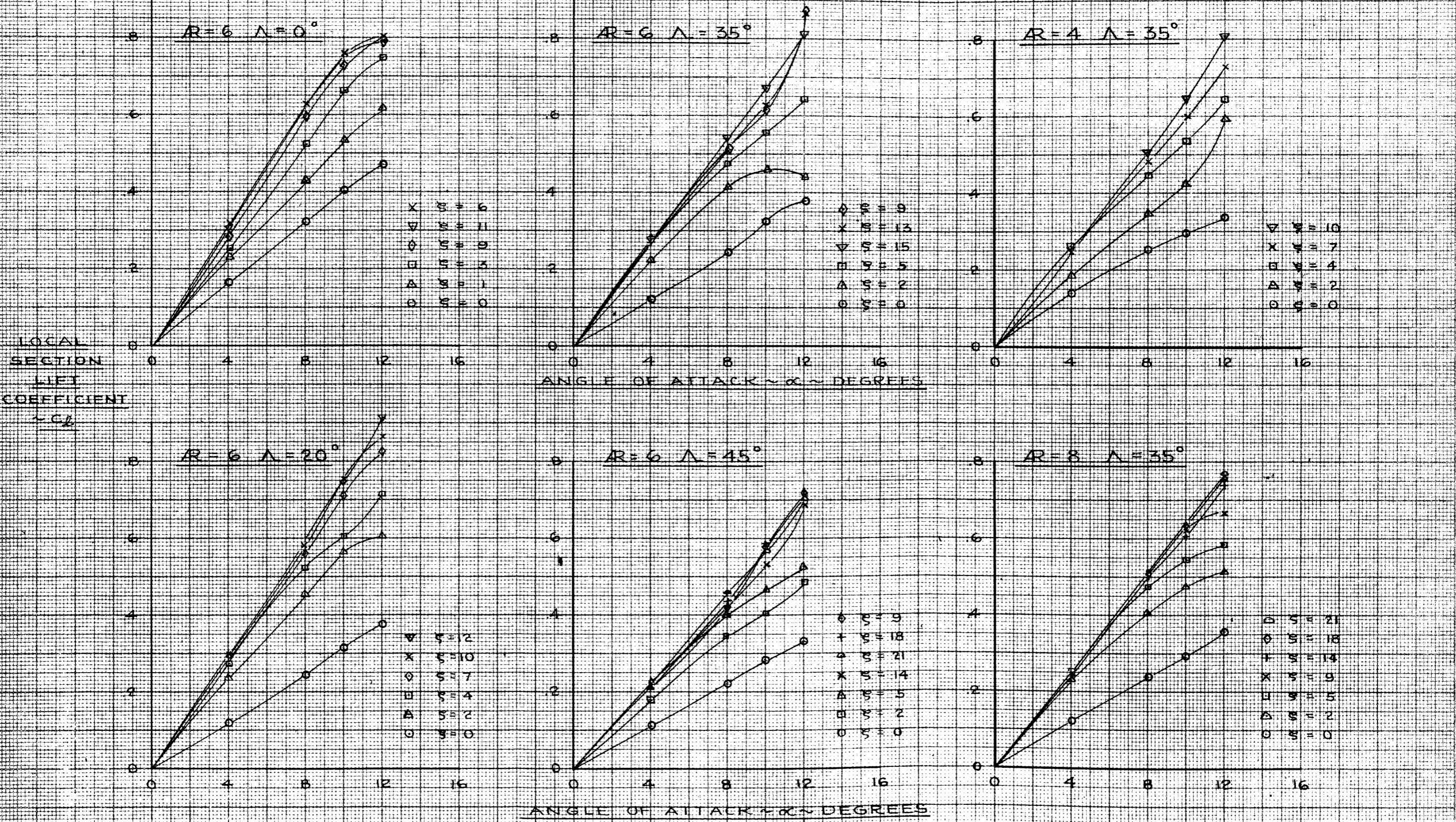
ANGLE OF ATTACK = 8°

ANGLE OF ATTACK = 12°



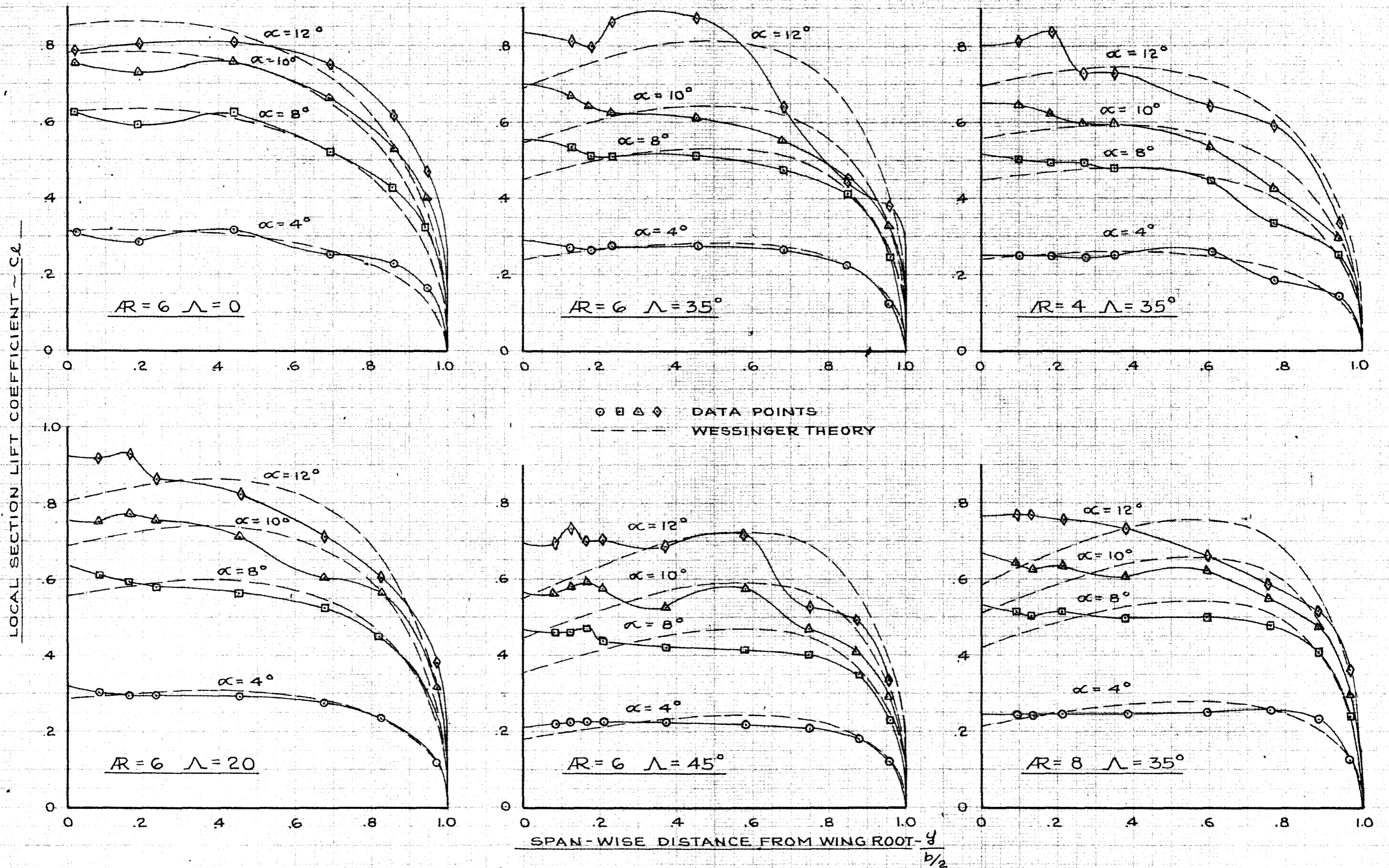
EFFECT OF ASPECT RATIO AND ANGLE OF ATTACK ON SURFACE PRESSURE DISTRIBUTION - SWEEPBACK =  $35^\circ$ ANGLE OF ATTACK =  $4^\circ$ ANGLE OF ATTACK =  $10^\circ$ ANGLE OF ATTACK =  $8^\circ$ ANGLE OF ATTACK =  $12^\circ$ 

# LOCAL SECTION LIFT CURVES

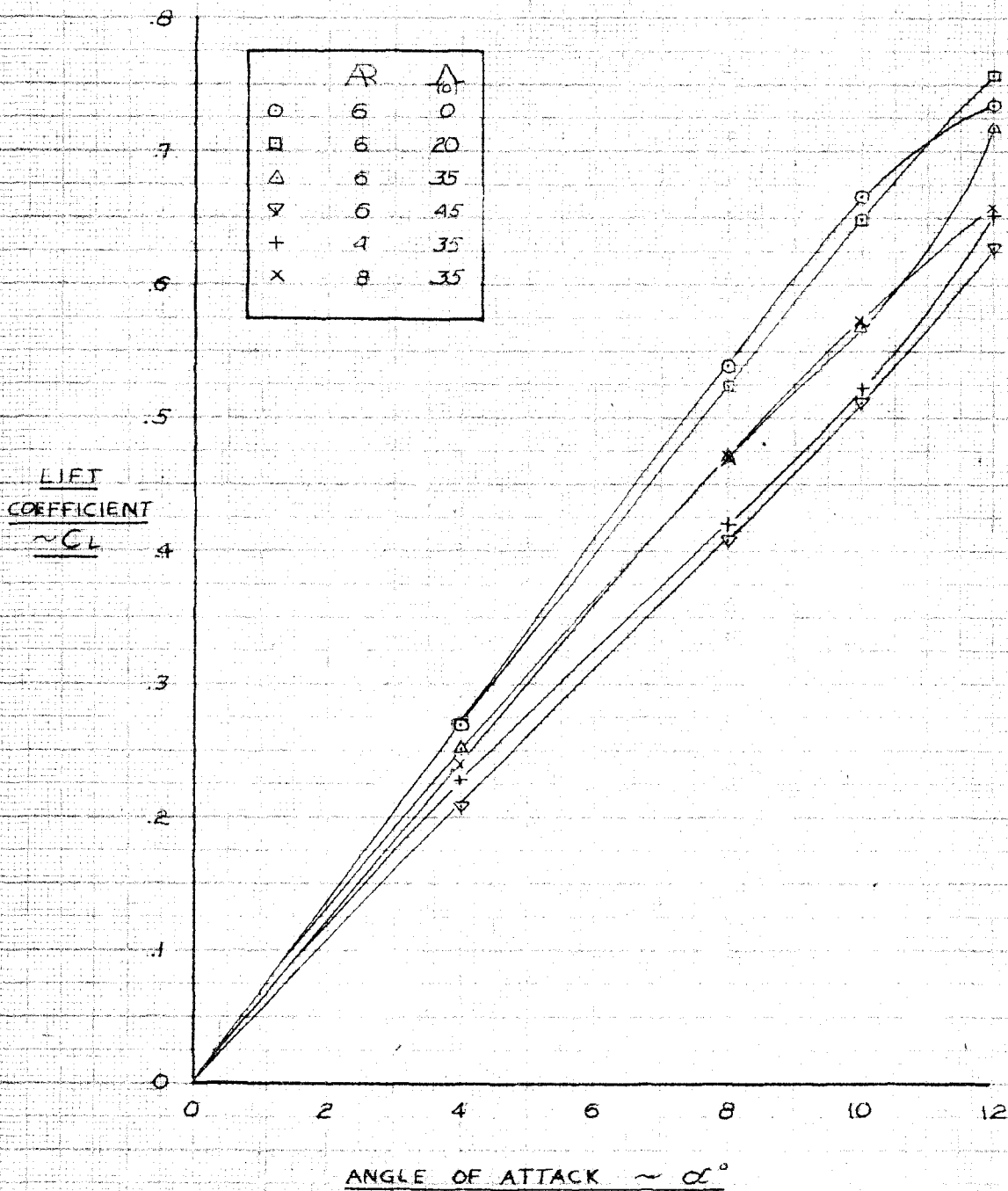




# SPAN-WISE DISTRIBUTION OF LIFT



# LIFT CURVES FOR VARIOUS WING PLANFORMS

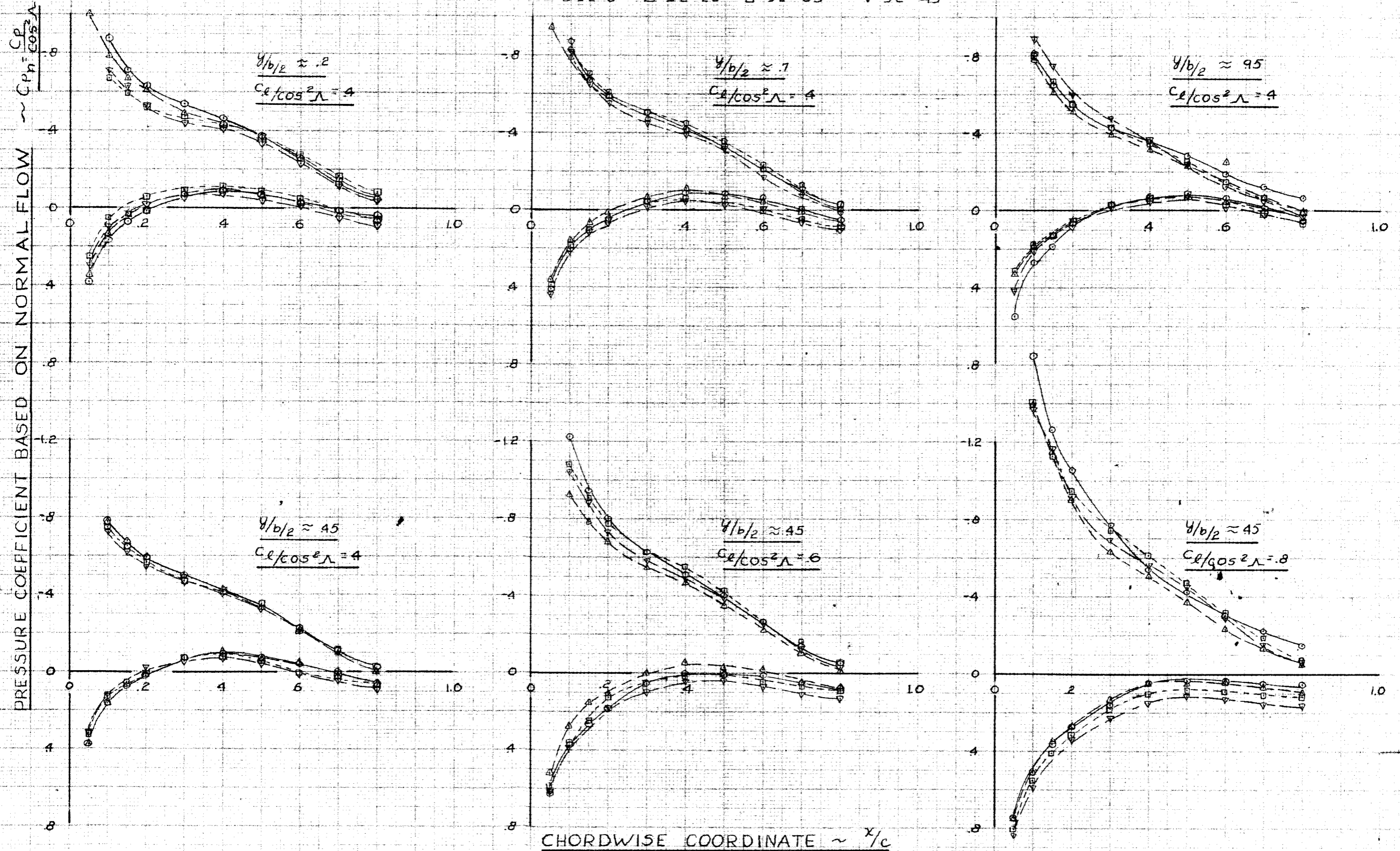


# RESOLUTION OF SURFACE PRESSURE DISTRIBUTION

EFFECT OF SWEEPBACK ON PRESSURE PATTERN BASED ON NORMAL COMPONENT OF FLOW

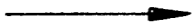

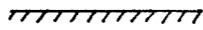
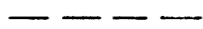

ASPECT RATIO = 6

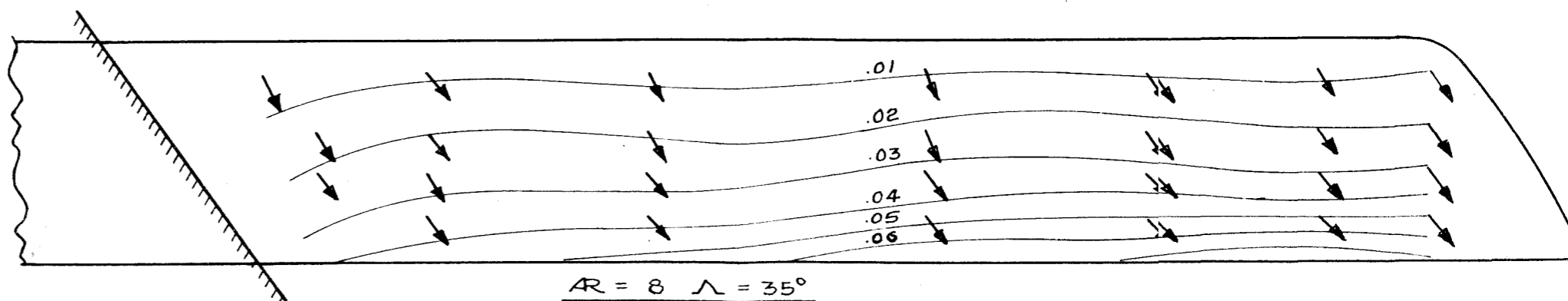
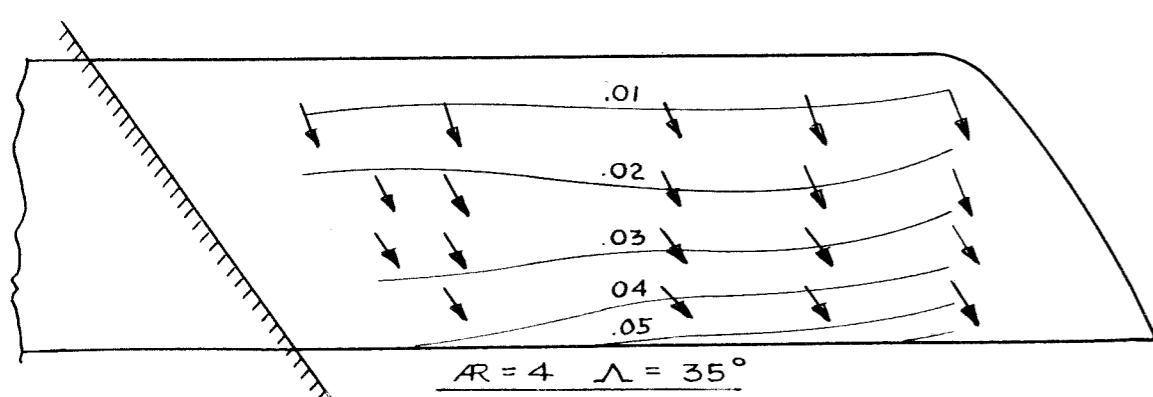
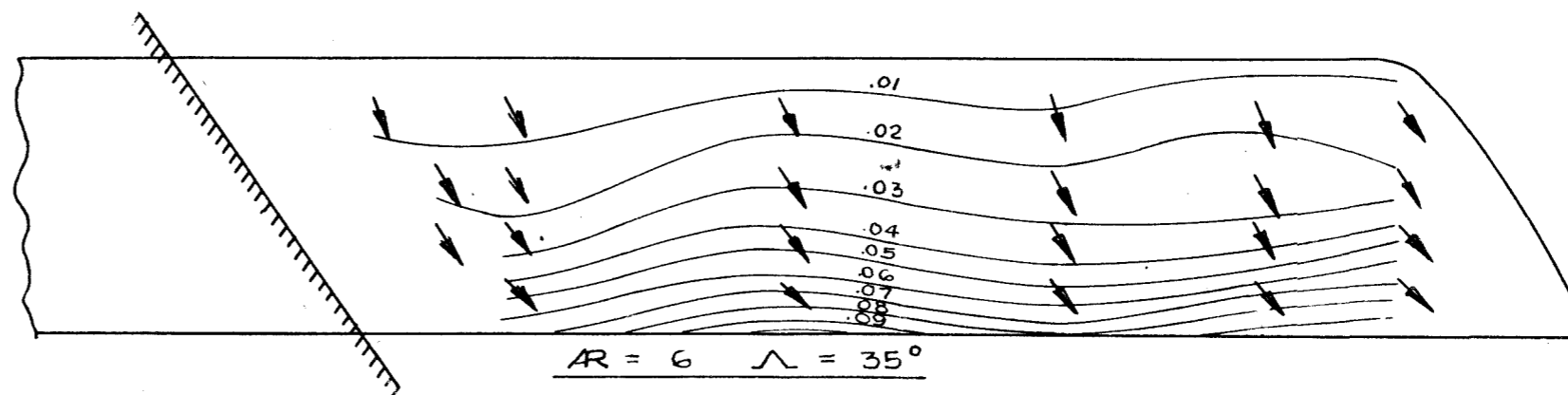
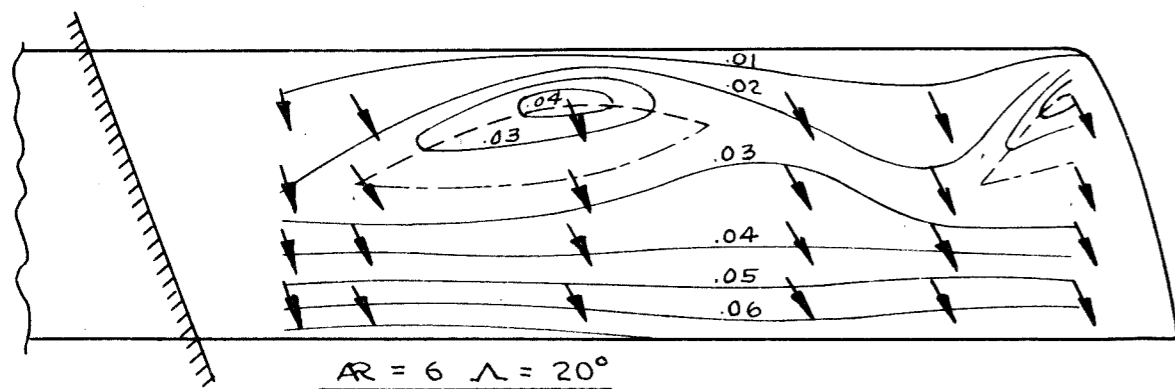
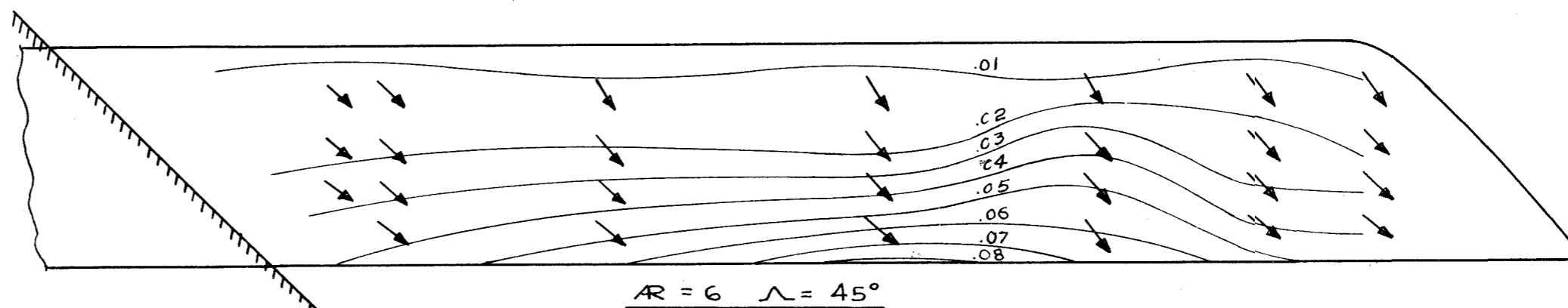
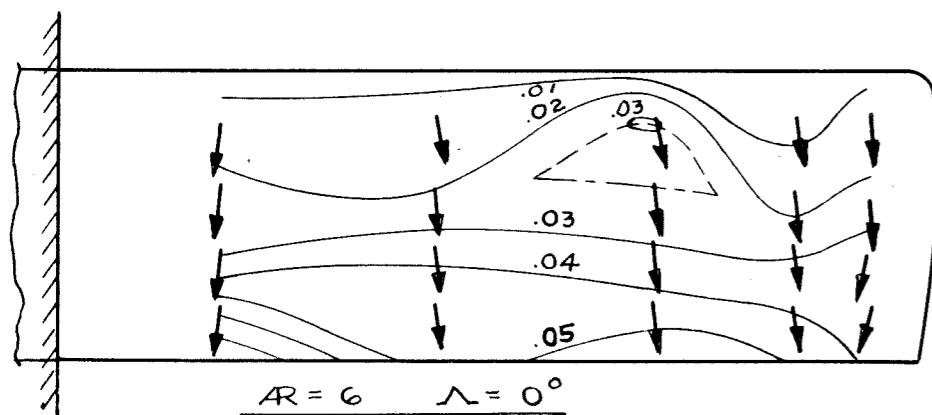
○  $\Lambda = 0^\circ$     △  $\Lambda = 20^\circ$     □  $\Lambda = 35^\circ$     ▽  $\Lambda = 45^\circ$



# BOUNDARY LAYER THICKNESS AND FLOW DIRECTION NEAR WING SURFACE

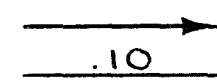
$\alpha = 4^\circ$

-  ARROW INDICATES FLOW DIRECTION AT 0.012 INCHES FROM WING SURFACE
-  .10 CONTOURS OF CONSTANT RESULTANT BOUNDARY LAYER DISPLACEMENT THICKNESS  $\delta_R^*$ , WITH THICKNESS LABELED IN INCHES
-  WIND TUNNEL WALL
-  CONTOURS OF LOCAL MAXIMUM  $\delta_R^*$
-  CONTOURS OF LOCAL MINIMUM  $\delta_R^*$

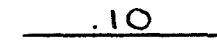


# BOUNDARY LAYER THICKNESS AND FLOW DIRECTION NEAR WING SURFACE

$$\alpha = 8^\circ$$

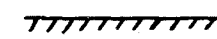


ARROW INDICATES FLOW DIRECTION AT 0.012 INCHES FROM WING SURFACE

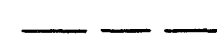


CONTOURS OF CONSTANT RESULTANT BOUNDARY LAYER DISPLACEMENT

THICKNESS,  $\delta_R^*$ , WITH THICKNESS LABELLED IN INCHES



WIND TUNNEL WALL



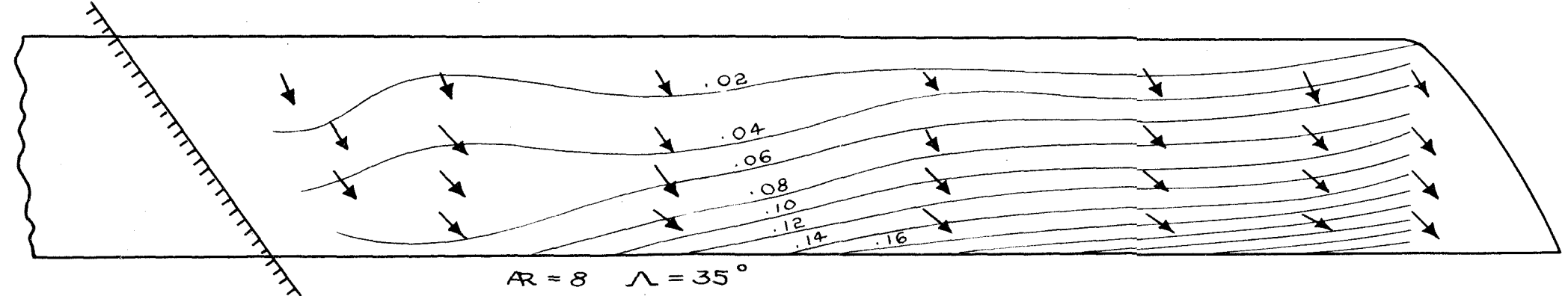
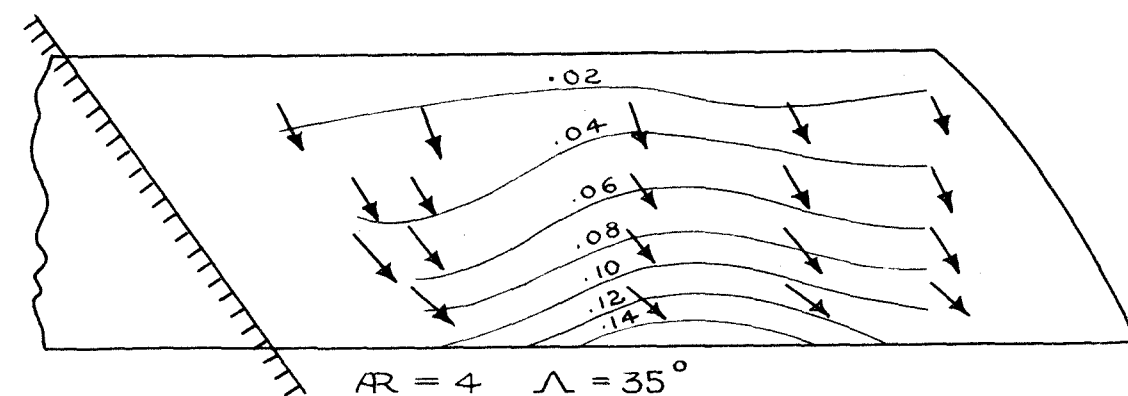
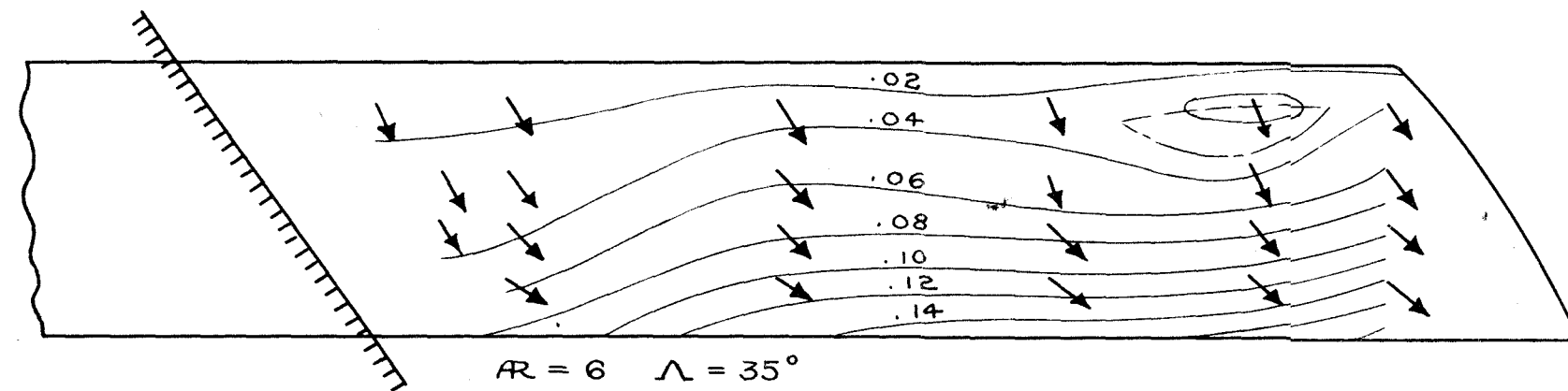
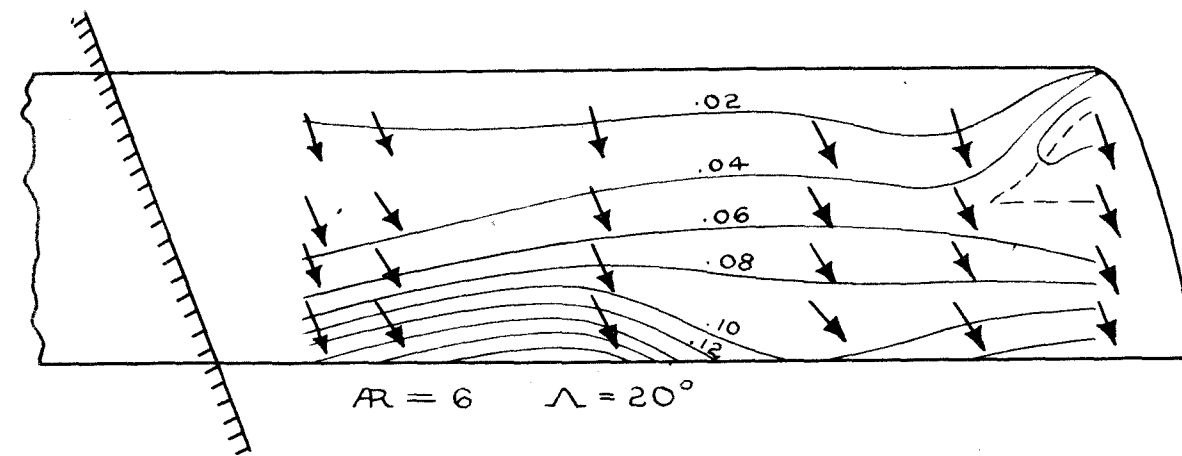
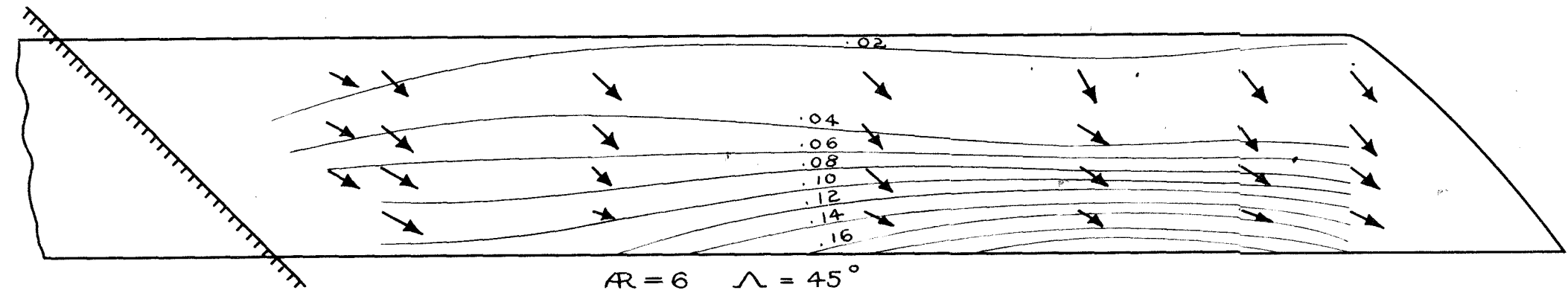
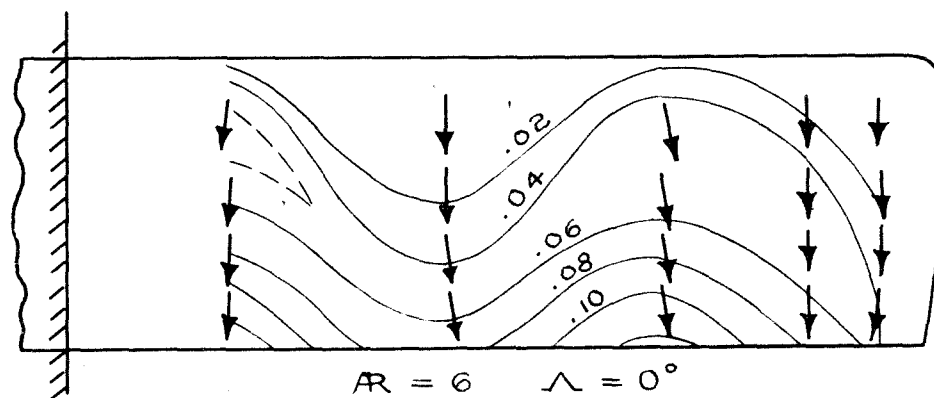
CONTOURS OF LOCAL MAXIMUM  $\delta_R^*$



CONTOURS OF LOCAL MINIMUM  $\delta_R^*$



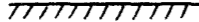
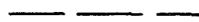




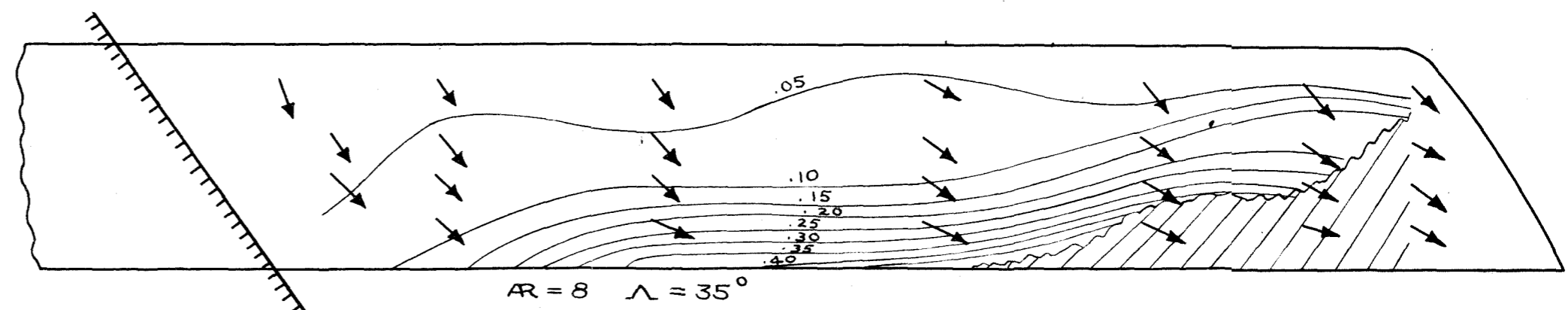
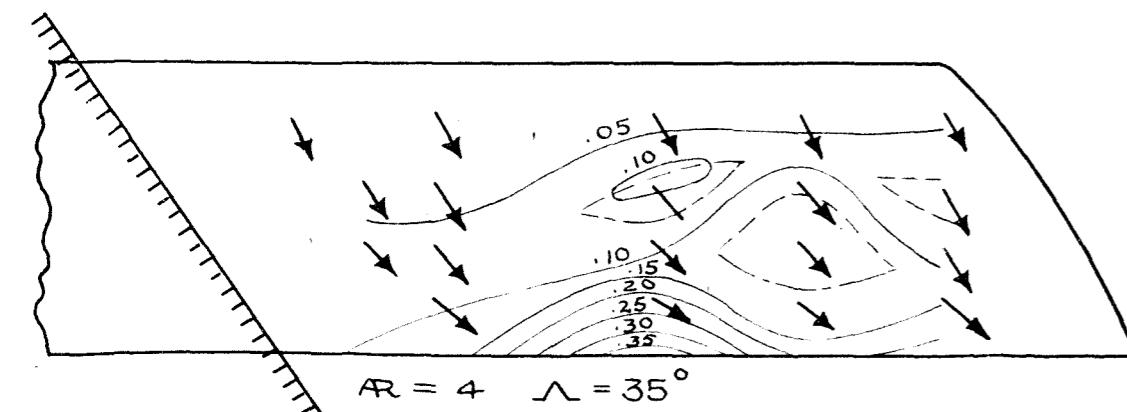
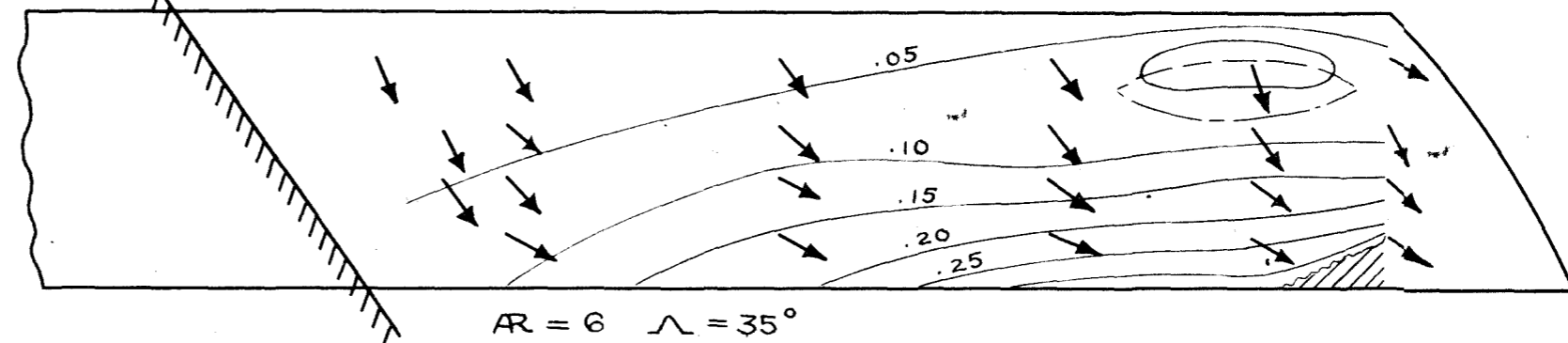
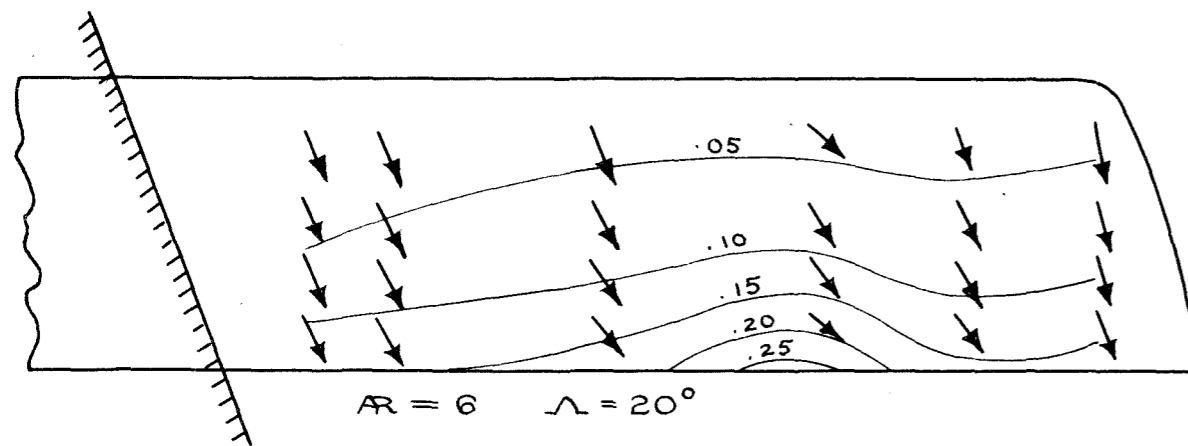
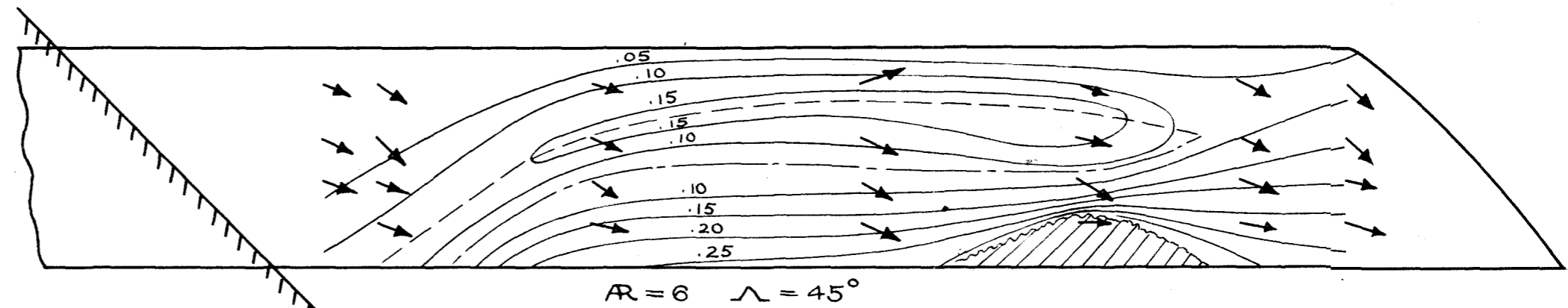
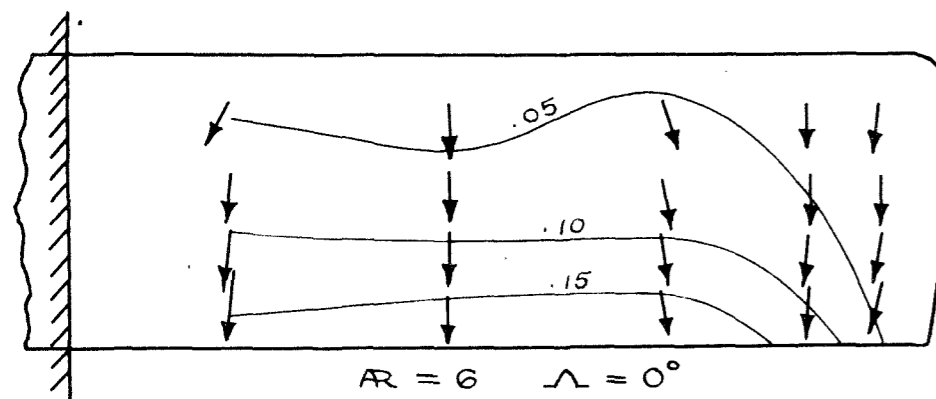
REGIONS OF SEPARATED FLOW



# BOUNDARY LAYER THICKNESS AND FLOW DIRECTION NEAR WING SURFACE




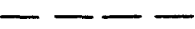


$$\alpha = 10^\circ$$

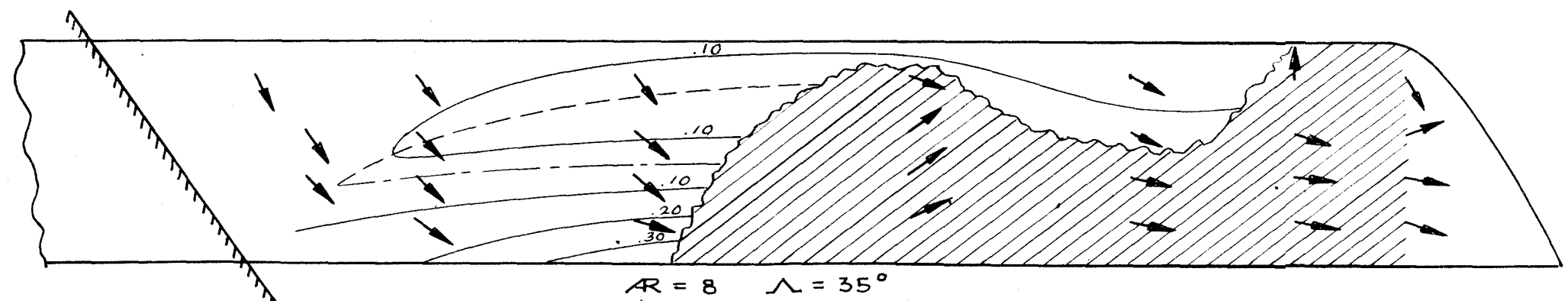
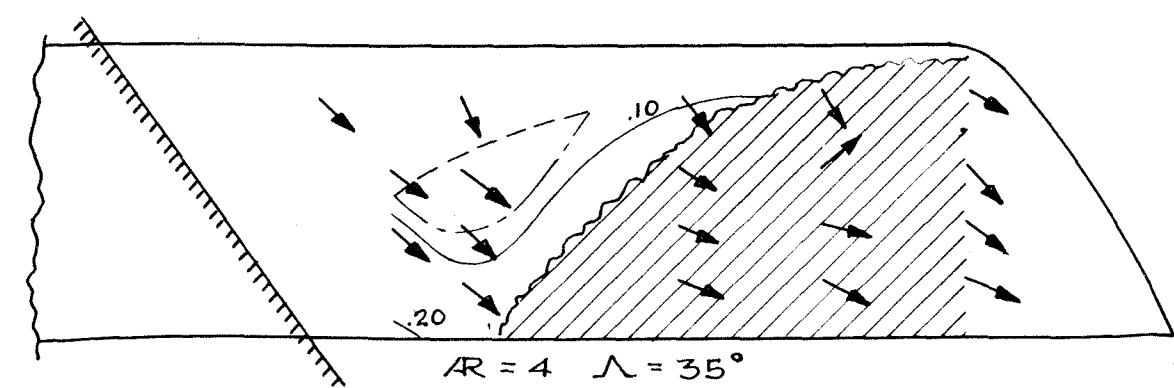
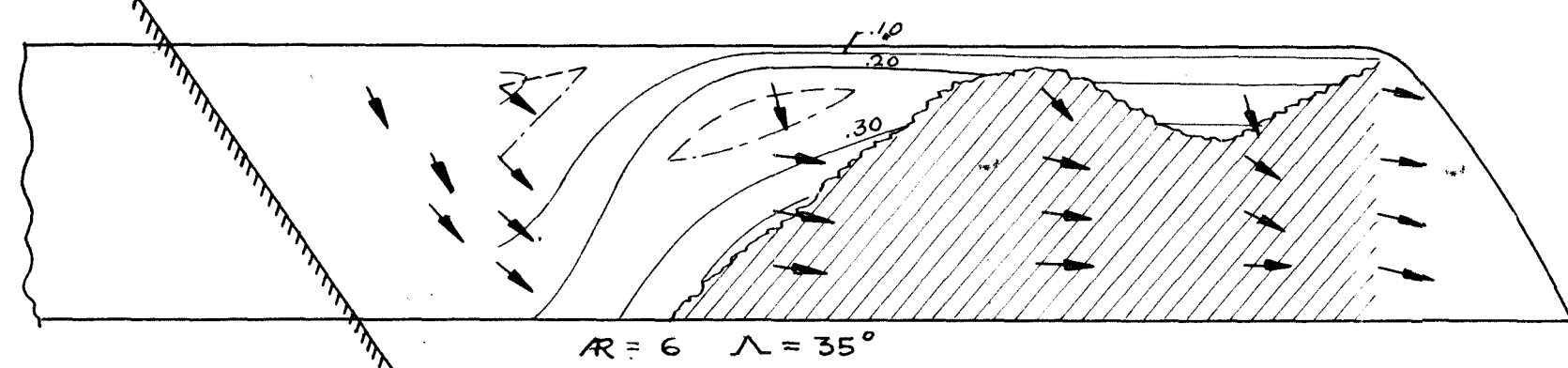
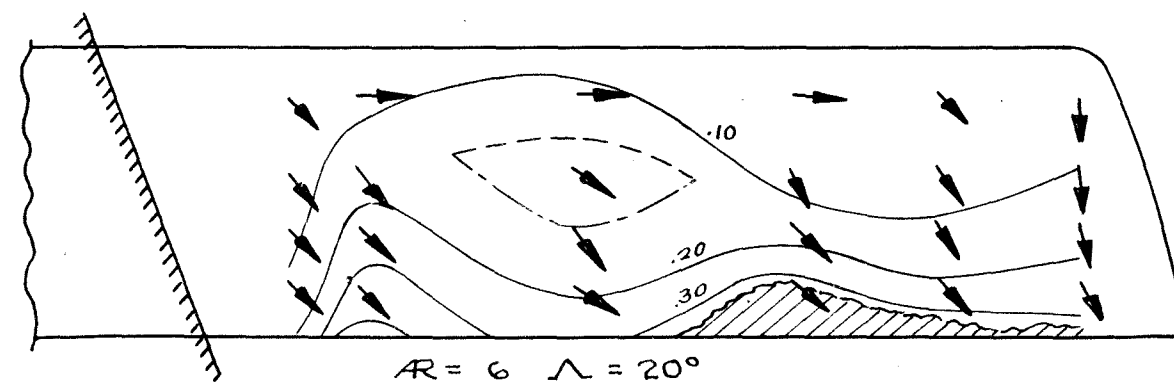
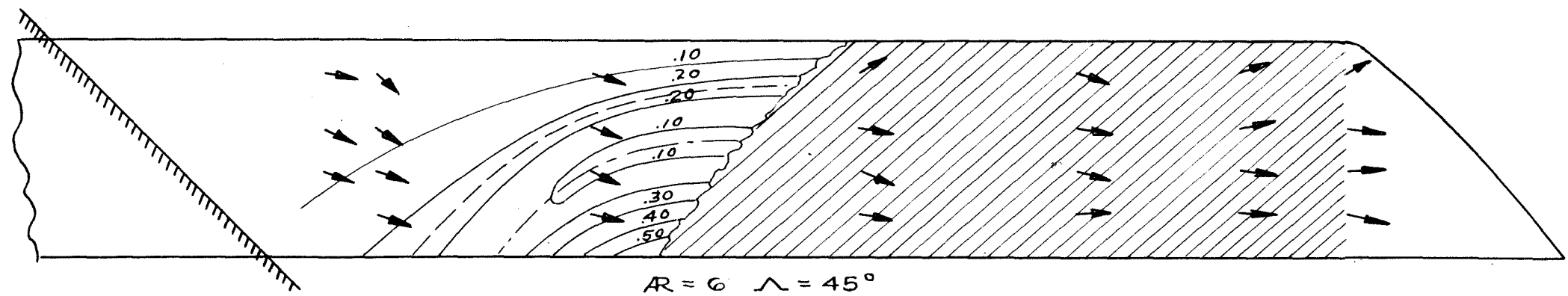
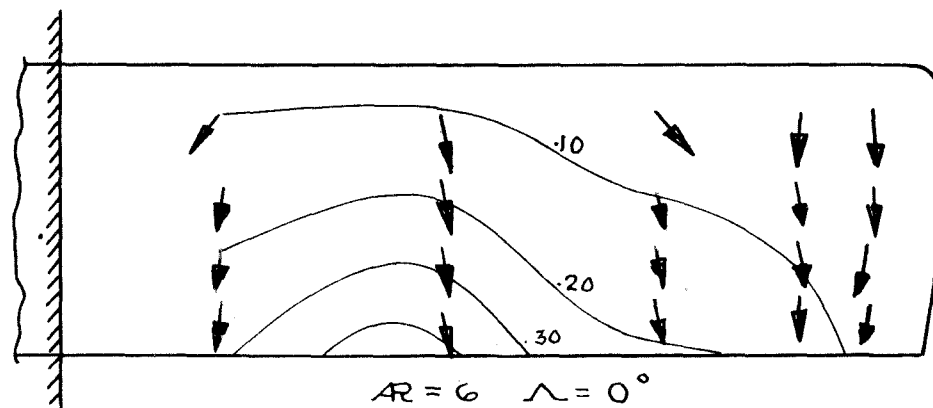
-  ARROW INDICATES FLOW DIRECTION AT 0.012 INCHES FROM WING SURFACE  
 .10 CONTOURS OF CONSTANT RESULTANT BOUNDARY LAYER DISPLACEMENT THICKNESS,  $\delta_R^*$ , WITH THICKNESS LABELED IN INCHES  
 WIND TUNNEL WALL  
 CONTOURS OF LOCAL MAXIMUM  $\delta_R^*$   
 CONTOURS OF LOCAL MINIMUM  $\delta_R^*$   
 REGIONS OF SEPARATED FLOW



# BOUNDARY LAYER THICKNESS AND FLOW DIRECTION NEAR WING SURFACE

$$\alpha = 12^\circ$$

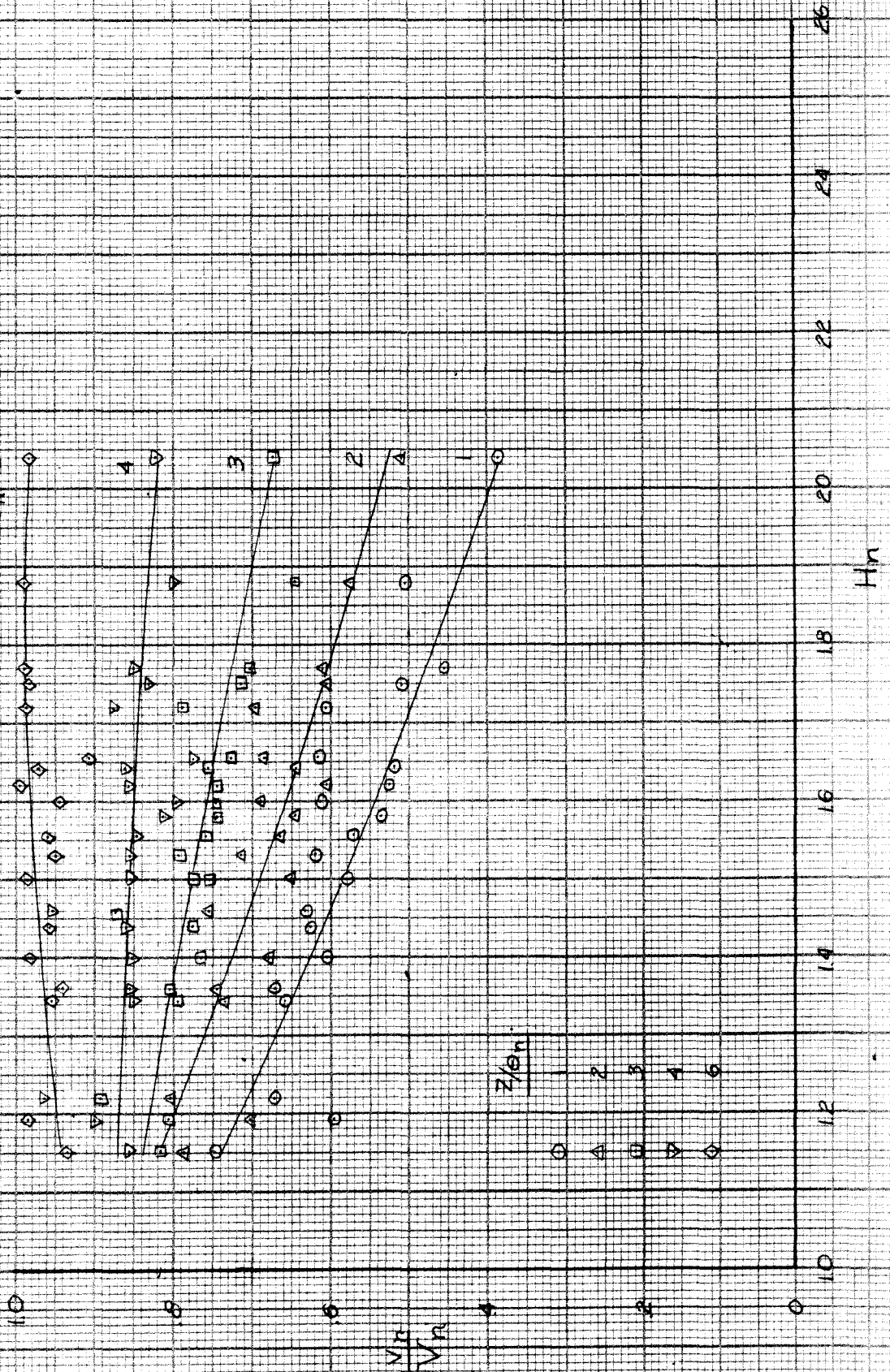
-  ARROW INDICATES FLOW DIRECTION AT 0.012 INCHES FROM WING SURFACE  
 .10 CONTOURS OF CONSTANT RESULTANT BOUNDARY LAYER DISPLACEMENT THICKNESS  $S_R^*$ , WITH THICKNESS LABELED IN INCHES  
 WIND TUNNEL WALL  
 CONTOURS OF LOCAL MAXIMUM  $S_R^*$   
 CONTOURS OF LOCAL MINIMUM  $S_R^*$   
 REGIONS OF SEPARATED FLOW



GENERALIZATION OF BOUNDARY LAYER PROFILE SHAPE

$\Lambda = 0^\circ$   $AR = 6$

$z/\delta_n = 6$

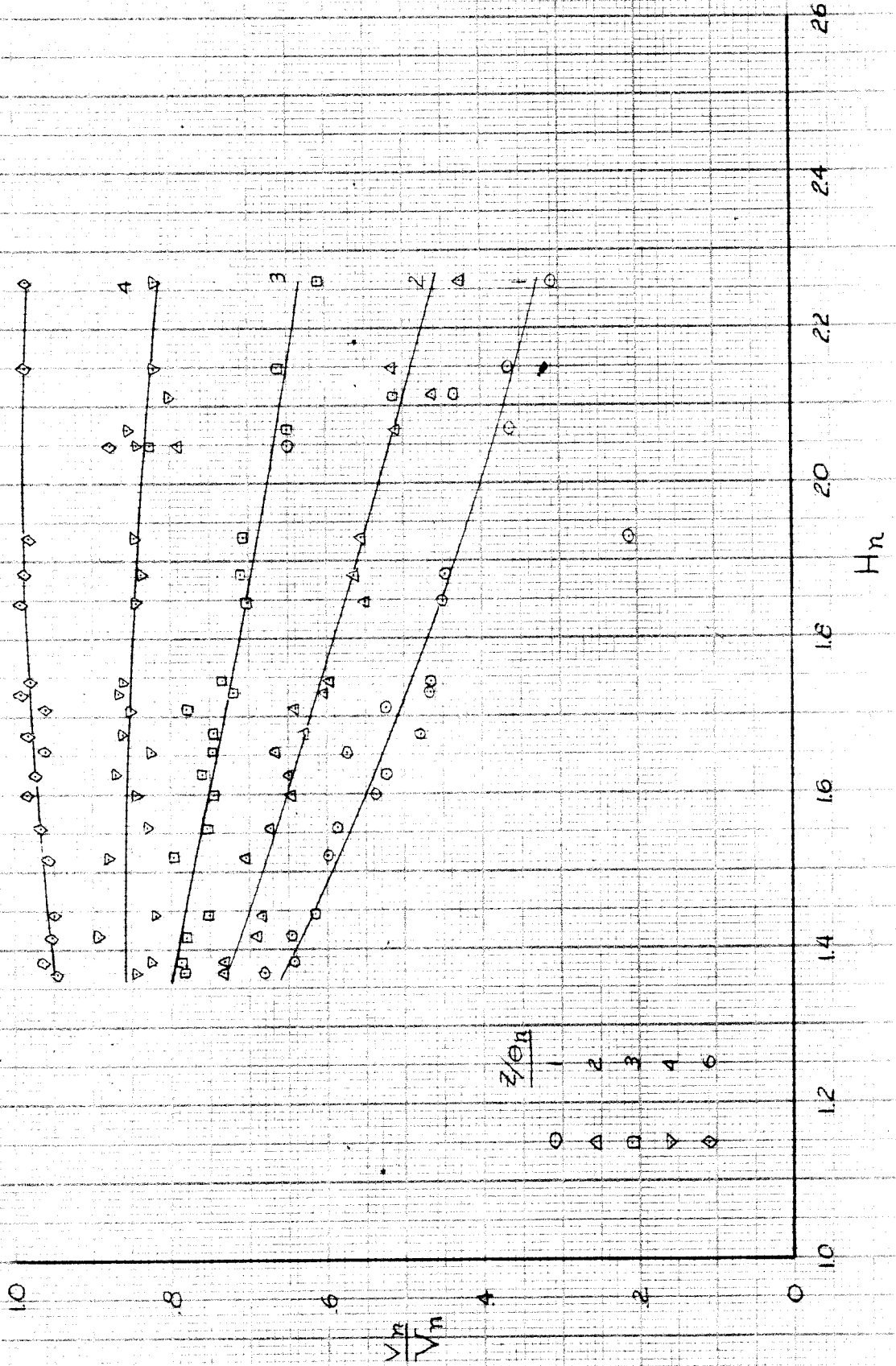




GENERALIZATION OF BOUNDARY LAYER PROFILE SHAPE

$\Lambda = 20^\circ$   $AR = 6$

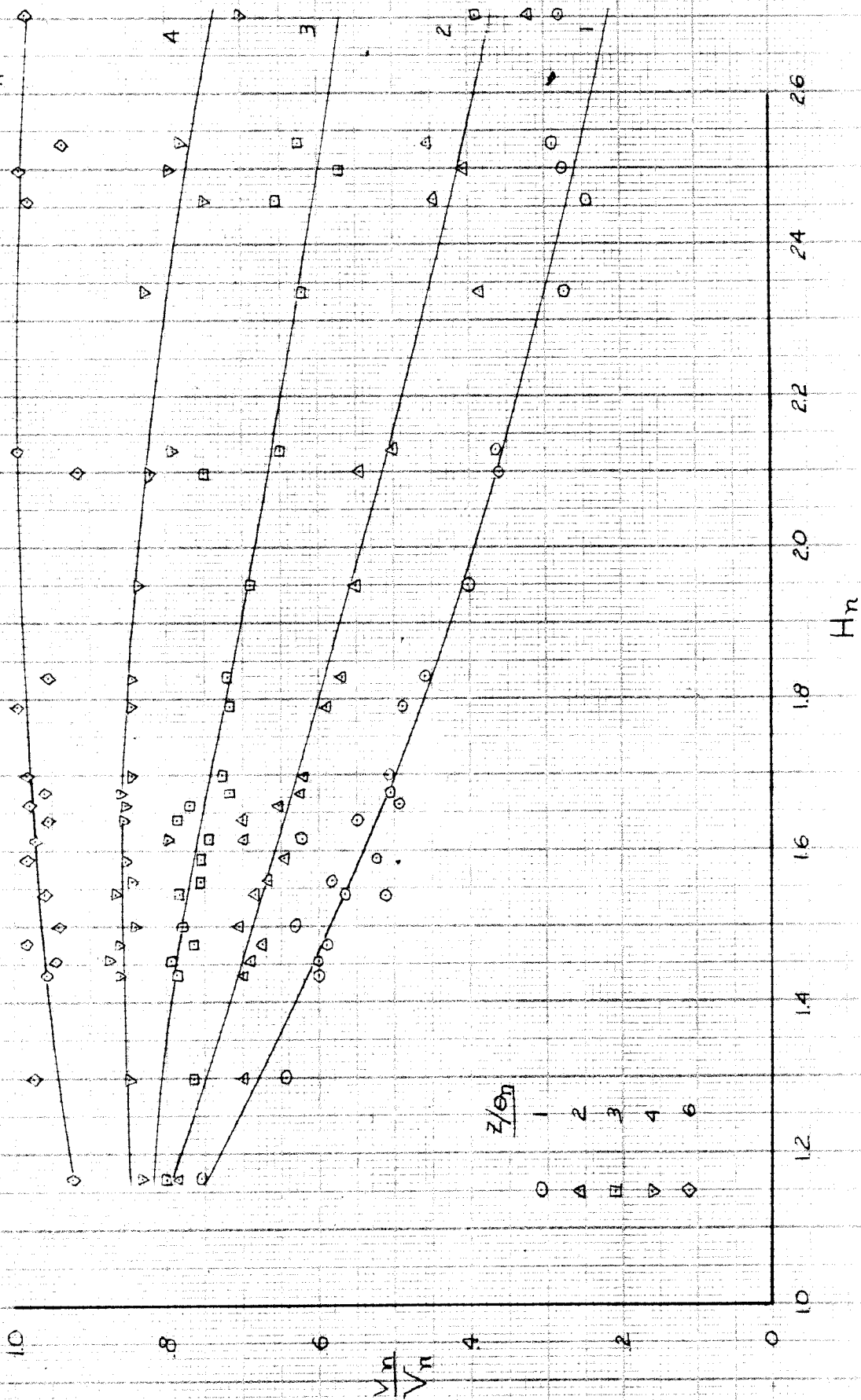
$z/\eta_n = 6$



# GENERALIZATION OF BOUNDARY LAYER PROFILE SHAPE

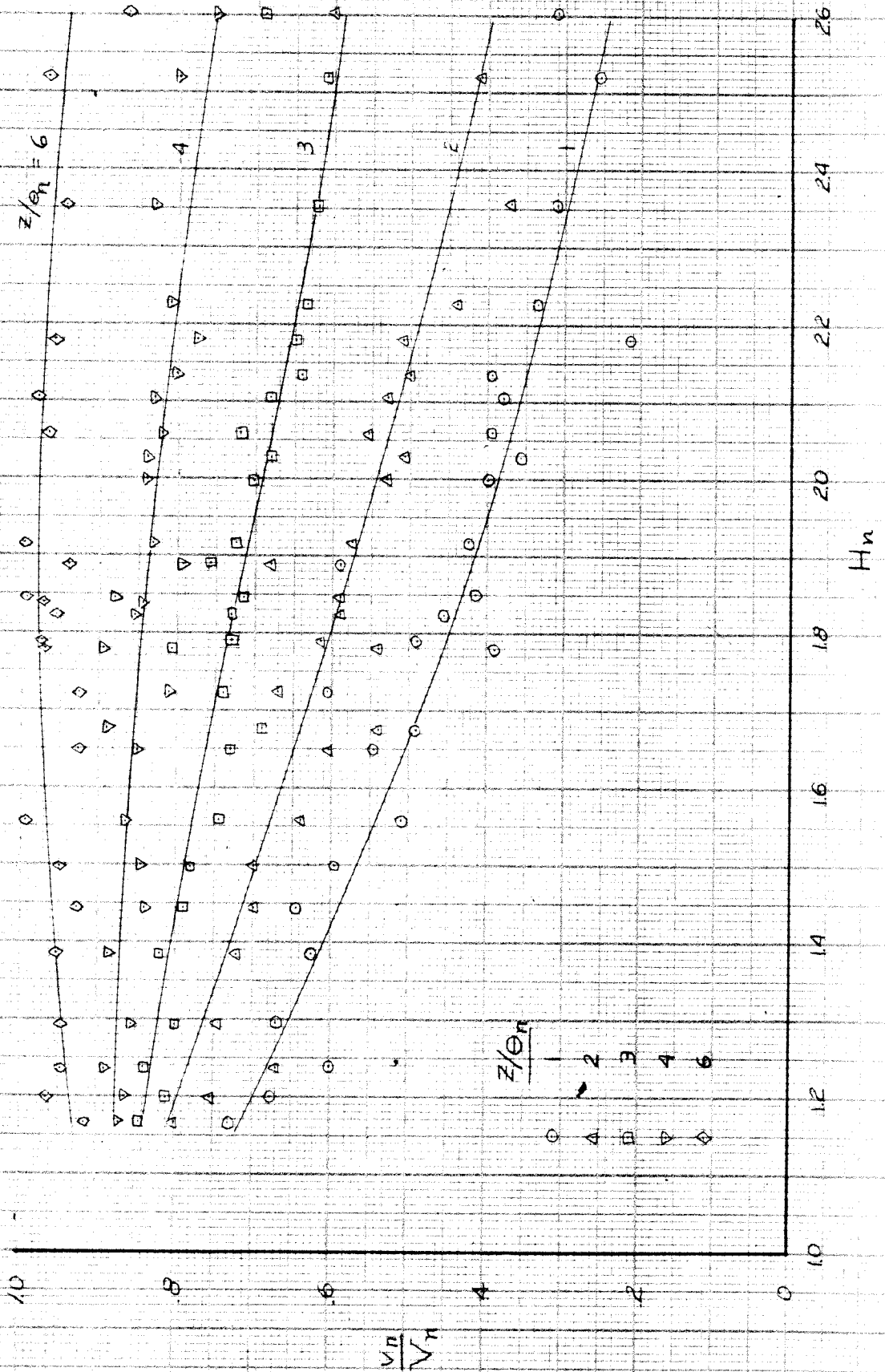
$\Lambda = 35^\circ$   $AR = 6$

$z/\theta_n = 6$



GENERALIZATION OF BOUNDARY LAYER PROFILE SHAPE

$\Lambda = 45^\circ$   $AR = 6$



EFFECT OF SWEEPBACK  
ON GENERALIZATION OF BOUNDARY LAYER PROFILE SHAPE

